Molecular-dynamics calculations of the velocity-autocorrelation function. Methods, hard-disk results

Jerome J. Erpenbeck and William W. Wood*
Los Alamos National Laboratory, Los Alamos, New Mexico 87545
(Received 29 January 1982)

The velocity-autocorrelation function $\rho_D(t)$ for hard disks is computed for ten values of the reduced volume, ranging from 30 to 1.4 times the close-packed volume (V_0) for systems of as few as 168 and as many as 5822 particles, by a Monte Carlo molecular-dynamics technique. For values of the time greater than roughly 20 mean-free times (t_0), the results are compared with the predictions of a version of the mode-coupling theory for $\rho_D(t)$, modified to take into account the finite size of the system. Except at the highest densities, the data agree with the modified theory when one uses Enskog values for the transport coefficients in evaluating the theoretical $\rho_D(t)$, provided the comparison is limited to times beyond a value $s_i t_0$, with s_i dependent on the density. The value of s_i appears to increase from roughly 20 at the lowest densities to 40 at a volume of $2V_0$. At volumes of 1.6, 1.5, and $1.4V_0$, the theoretical $\rho_D(t)$'s are too large out to times as large as $320t_0$, unless we use values of the transport coefficients rather larger than the Enskog values in evaluating the theoretical $\rho_D(t)$. The velocity-autocorrelation-function results for $t < 20t_0$ are presented as the difference relative to the Lorentz-Boltzmann-Enskog prediction, which has the exact slope at $t=0$.

I. INTRODUCTION

Alder and Wainwright[1] first demonstrated, by molecular-dynamics (MD) calculations, the slow decay of the velocity-autocorrelation function $\rho_D(t)$ for hard spheres and disks, suggesting the long-time decay law

$$\rho_D(t) \sim \alpha_D (t/t_0)^{-d/2} , \tag{1.1}$$

where t is the dynamical time, t_0 is the mean-free time, d is the dimensionality (2 or 3), and α_D is a density-dependent coefficient. Subsequently, this formula was established theoretically, from the kinetic theory by Dorfman and Cohen,[2] and from hydrodynamic mode-coupling theory by Ernst, Hauge, and van Leeuwen,[3,4] by Kawasaki,[5] and by Pomeau[6]; see also the review by Pomeau and Resibois.[7]

While the asymptotic result then, appears to be firmly established, the observations by Alder and Wainwright were, in fact, quite limited, particularly in three dimensions for which a single observation of $\rho_D(t)$ (i.e., for a single value of the density) as a function of t indicating $t^{-3/2}$ decay was reported. Moreover, the coefficient α_D observed for hard spheres was later discovered[8] to differ by an apparently significant amount from the theoretical value. In view of the importance of Eq. (1.1) in the theory of transport, we felt it worthwhile to confirm and, if possible, extend the Alder-Wainwright results. This project was begun some years ago and a number of the results have been reported previously, by us[8–11] as well as by others.[12–19] It is our purpose here to describe our calculations in detail and to present our results for hard disks. The results for hard spheres will be presented in a subsequent publication.

After describing the system and giving the formulas for the time-correlation functions for self-diffusion in Sec. II, we rederive in Sec. III the mode-coupling theory of Ernst, Hauge, and van Leeuwen[3] (EHvL) but for a finite periodic system in the expectation that at least some aspects of the dependence of the numerical results on the size of the system will thereby be taken into account. It is this modification of the theory with which the numerical results are compared. In Sec. IV we describe the Monte Carlo, molecular-dynamics (MCMD) method used to generate the numerical data and define the reduced quantities which are actually reported. In Sec. V we consider several questions regarding the numerical methods, including (1) the method of evaluation of the velocity-autocorrelation function (VACF), (2) the statistical

comparison of the time-correlation function data, either with theory or with another set of data, and (3) the effects of trajectory precision on the results. The VACF's for hard disks are presented graphically in Sec. VI for long times and compared with the modified EHvL theory. Finally in Sec. VII the short- and intermediate-time data are presented in the form of the difference between the MCMD results and the Lorentz-Boltzmann-Enskog theory.

II. GREEN-KUBO FORMULA

The system consists of N identical particles of mass m in a d-dimensional volume V, with positions $\underline{r}^N=(\vec{r}_1,\vec{r}_2,\ldots,\vec{r}_N)$ and velocities $\underline{v}^N=(\vec{v}_1,\vec{v}_2,\ldots,\vec{v}_N)$. In order to minimize finite-system effects, periodic boundary conditions are imposed, whereby the volume V is of such a shape that translations of the volume along d linearly independent axes fill all of the space with replications of the N-particle system in V. For simplicity we assume these translational axes coincide with the Euclidean axes $\hat{e}_1,\hat{e}_2,\ldots,\hat{e}_d$ (where the caret denotes a unit vector) and denote the corresponding edge lengths by $L_1,L_2,\ldots,L_d$, respectively, so that $L_1L_2\cdots L_d=V$.

The potential energy of the system $U(\underline{r}^N)$ will, in general, have a contribution from each replication of the N particles in volume V,

$$U(\underline{r}^N)=\sum_{\vec{\nu}} U_{\vec{\nu}}(\underline{r}^N) ,$$
$$\sum_{\vec{\nu}}=\sum_{\nu_1}\sum_{\nu_2}\cdots\sum_{\nu_d} , \tag{2.1}$$

where the ν_i are integers identifying a particular periodic image and the ν_i sums extend from $-\infty$ to $+\infty$. For the familiar case of pairwise-additive interactions $u(\vec{r})$,

$$U_{\vec{\nu}}(\underline{r}^N)=\tfrac{1}{2}\sum_{i=1}^{N}\sum_{j\neq i} u(\vec{r}_{ij}+\vec{L}_{\vec{\nu}}) ,$$
$$\sum_{j\neq i}=\sum_{j=1}^{N}{}' , \tag{2.2}$$
$$\vec{L}_{\vec{\nu}}=\sum_{k=1}^{d}\nu_k L_k\hat{e}_k ,$$

where $\vec{r}_{ij}=\vec{r}_i-\vec{r}_j$ and the prime indicates the absence of the $j=i$ term in the j sum.

The Green-Kubo formula for the self-diffusion coefficient is given by

$$D=\lim_{t\to\infty} \mathrm{T\,lim} D(t) , \tag{2.3a}$$

$$D(t)=\int_0^t dt'\rho_D(t') , \tag{2.3b}$$

$$\rho_D(t)=\langle u_{1x}(0)u_{1x}(t)\rangle , \tag{2.3c}$$

where t is the dynamical time, T lim denotes the thermodynamic limit, and $\vec{u}_i$ is the velocity in the center-of-mass frame of reference

$$\vec{u}_i(t)=\vec{v}_i(t)-\vec{P}/Nm ,$$
$$\vec{P}=m\sum_{i=1}^{N}\vec{v}_i(t) . \tag{2.4}$$

Note, however, that $\vec{P}$ is independent of the time by virtue of the conservation of linear momentum in the system. The angular brackets denote an ensemble average over the phase $\underline{x}^N=(\underline{r}^N,\underline{v}^N)$, which is the initial phase for the dynamical trajectory $\underline{x}^N(t)$, i.e., $\underline{x}^N(0)=\underline{x}^N$. The symbol β is dependent on the statistical ensemble. For the canonical ensemble it denotes $1/k_BT$, with k_B the Boltzmann constant and T the thermodynamic temperature. For the microcanonical ensemble $\beta=dN/2E$, with E the internal energy. The appearance of the velocity $\vec{u}_i$ in the center-of-mass frame of reference rather than the $\vec{v}_i$ is a matter of some importance in the numerical calculations, although the distinction is of no consequence in the thermodynamic limit. Indeed, because of the conservation of linear momentum, one obtains

$$\rho_D(t)=c_D(t)-\langle P^2\rangle/N^2m^2 ,$$
$$c_D(t)=\langle v_{1x}(0)v_{1x}(t)\rangle , \tag{2.5}$$
$$\langle P^2\rangle=Nm^2\langle v_{1x}^2\rangle ,$$

so that one can readily calculate either form of the VACF from the other.

In order to complete our specification of the trajectory $\underline{x}^N(t)$, we define the $\vec{r}_i(t)$ to be the position of particle i at time t in the *infinite-checkerboard* version of the periodic system[10] so that the $\vec{r}_i(t)$ are continuous and identical to the integral of the velocities $\vec{v}_i(t)$. The initial positions $\vec{r}_i(0)$ however, will be assumed to lie in the $\vec{\nu}=0$ cell.

III. MODE-COUPLING THEORY FOR FINITE N

An ever-present problem in both Monte Carlo (MC) and molecular-dynamics calculations arises from the small number of particles which can be treated numerically. Since one can perform these calculations with at most several thousand particles, considerable care is required in extracting the

large-system limit of a calculated quantity. It appears that for time-correlation functions this problem is particularly severe, for Alder and Wainwright[1] report that for times t of the order of the acoustic-wave traversal time $t_a = L/c$ where L is the shortest edge length of the system and c is the sound speed, $\rho_D(t)$ is strongly affected by the finite size of the system. If, then, one requires $\rho_D(t)$ for large values of the time, say t as large as t_m, one must either calculate for a large enough system so that $t_a > t_m$, or have at hand some means of correcting for finite-system effects. Here we apply the Ernst, Hauge, and van Leeuwen[3] theory to a finite periodic system, using the canonical ensemble, to obtain a version of the theory for finite systems. Several comparisons between our molecular-dynamics results and this modification of the theory have been reported previously.[8,9] An attempt to modify the EHvL theory for finite systems was also reported by Keyes and Ladanyi,[20] but their theory is, as we shall see, incomplete.

A. VACF as nonequilibrium average

We follow EHvL in computing $c_D(t)$, Eq. (2.5), by decomposing the canonical ensemble average into a subensemble average characterized by a given velocity $\vec{v}_0$ of a tagged particle (particle 1) and a given distribution $W(\vec{r}_1-\vec{r}_0)$ of the tagged particle about a point $\vec{r}_0$, viz.,

$$c_D(t)=\int_V d\vec{r}_0 \int d\vec{v}_0 v_{0x} \langle v_{1x}(t)\delta(\vec{v}_1-\vec{v}_0) \times W(\vec{r}_1-\vec{r}_0)\rangle \tag{3.1}$$

which is evidently true provided $W(\vec{r})$ is normalized in V and is periodic,

$$W(\vec{r}+\vec{L}_{\vec{\nu}})=W(\vec{r}) . \tag{3.2}$$

Write the ensemble average in Eq. (3.1) as a nonequilibrium ensemble average (indicated by a subscript n) through the definition, for an arbitrary phase function $f(\underline{x}^N)$

$$\langle f(\underline{x}^N)\rangle_n = \frac{\langle f(\underline{x}^N)\delta(\vec{v}_1-\vec{v}_0)W(\vec{r}_1-\vec{r}_0)\rangle}{\langle \delta(\vec{v}_1-\vec{v}_0)W(\vec{r}_1-\vec{r}_0)\rangle} \tag{3.3}$$

in which the dependence of the left-hand side on $\vec{r}_0$ and $\vec{v}_0$ is suppressed. We compute the denominator for the canonical ensemble

$$\begin{aligned}
&\langle \delta(\vec{v}_1-\vec{v}_0)W(\vec{r}_1-\vec{r}_0)\rangle \\
&\quad = \int d\underline{x}^N \rho_N(\underline{x}^N)\delta(\vec{v}_1-\vec{v}_0)W(\vec{r}_1-\vec{r}_0) , \\
&\rho_N(\underline{x}^N)=g_N(\underline{r}^N)\prod_{i=1}^{N}\varphi_0(v_i) , \\
&g_N(\underline{r}^N)=Q(N,V,T)^{-1}\exp[-\beta U(\underline{r}^N)] , \\
&Q(N,V,T)=\int_V d\underline{r}^N \exp[-\beta U(\underline{r}^N)] , \\
&\varphi_0(v)=\left[\frac{m\beta}{2\pi}\right]^{d/2}\exp(-m\beta v^2/2) ,
\end{aligned} \tag{3.4}$$

to be

$$\langle \delta(\vec{v}_1-\vec{v}_0)W(\vec{r}_1-\vec{r}_0)\rangle = V^{-1}\varphi_0(v_0) \tag{3.5}$$

whence we obtain from Eqs. (3.1) and (3.3),

$$c_D(t)=V^{-1}\int_V d\vec{r}_0 \int d\vec{v}_0 \varphi_0(v_0) v_{0x} \times \langle v_{1x}(t)\rangle_n . \tag{3.6}$$

B. Transition to hydrodynamics

In order to bring Eq. (3.6) into a form in which hydrodynamic concepts can be applied, we compute the tagged-particle distribution function in the nonequilibrium ensemble

$$f^{(s)}(\vec{r},\vec{v},t) = \left\langle \sum_{\vec{\nu}} \delta(\vec{r}_1(t)-\vec{L}_{\vec{\nu}}-\vec{r})\delta(\vec{v}_1(t)-\vec{v})\right\rangle_n , \tag{3.7}$$

where the sum over $\vec{\nu}$ accounts for the contribution from each replication of the $\vec{\nu}=0$ cell. For a given initial phase $\underline{x}^N$ and a given time t, at most a single $\vec{\nu}$ would contribute to the right-hand side. Computing then the average of v_x over the distribution $f^{(s)}$ and comparing with Eq. (3.3), one obtains

$$\langle v_{1x}(t)\rangle_n = \int_V d\vec{r} \int d\vec{v} f^{(s)}(\vec{r},\vec{v},t) v_x . \tag{3.8}$$

Equations (3.6) and (3.8) for the velocity-autocorrelation function are exact, but require knowledge of the tagged-particle distribution function to be useful. Following EHvL, we evaluate the latter approximately from hydrodynamics. In particular, we use the EHvL assumption I that the tagged-particle distribution function and the single-particle distribution function

$$f(\vec{r},\vec{v},t)=\left\langle \sum_{\vec{\nu}}\sum_{i=1}^{N} \delta(\vec{r}_i(t)-\vec{L}_{\vec{\nu}}-\vec{r})\delta(\vec{v}_i(t)-\vec{v})\right\rangle_n \tag{3.9}$$

approach the local-equilibrium distributions quickly compared with the rate of decay of the autocorrelation function $c_D(t)$. By this assumption, then, we write $f^{(s)}(\vec{r},\vec{v},t)\sim f_l^{(s)}(\vec{r},\vec{v},t)$ and $f(\vec{r},\vec{v},t)\sim f_l(\vec{r},\vec{v},t)$, where the local-equilibrium distribution functions are

$$f_l(\vec{r},\vec{v},t)=n(\vec{r},t)\left[\frac{m}{2\pi k_B T(\vec{r},t)}\right]^{d/2}\exp\left[-\frac{m}{2\pi k_B T(\vec{r},t)}[\vec{v}-\vec{u}(\vec{r},t)]^2\right],$$
$$f_l^{(s)}(\vec{r},\vec{v},t)=P(\vec{r},t)\left[\frac{m}{2\pi k_B T(\vec{r},t)}\right]^{d/2}\exp\left[-\frac{m}{2\pi k_B T(\vec{r},t)}[\vec{v}-\vec{u}(\vec{r},t)]^2\right], \tag{3.10}$$

in which $n(\vec{r},t)$, $P(\vec{r},t)$, $\vec{u}(\vec{r},t)$, and $T(\vec{r},t)$ are the hydrodynamic fields of number density, tagged-particle density, mass velocity, and temperature, respectively,

$$n(\vec{r},t)=\left\langle\sum_{\vec{\nu}}\sum_{i=1}^{N}\delta(\vec{r}_i(t)-\vec{L}_{\vec{\nu}}-\vec{r})\right\rangle_n, \tag{3.11a}$$

$$n(\vec{r},t)\vec{u}(\vec{r},t)=\left\langle\sum_{\vec{\nu}}\sum_{i=1}^{N}\delta(\vec{r}_i(t)-\vec{L}_{\vec{\nu}}-\vec{r})\vec{v}_i(t)\right\rangle_n, \tag{3.11b}$$

$$P(\vec{r},t)=\left\langle\sum_{\vec{\nu}}\delta(\vec{r}_1(t)-\vec{L}_{\vec{\nu}}-\vec{r})\right\rangle_n, \tag{3.11c}$$

with $T(\vec{r},t)$ obtained from $n(\vec{r},t)$ and the energy density

$$e(\vec{r},t)=\left\langle\sum_{\vec{\nu}}\sum_{i=1}^{N}\delta(\vec{r}_i(t)-\vec{L}_{\vec{\nu}}-\vec{r})e_i(t)\right\rangle_n,$$
$$e_i(t)=\tfrac{1}{2}mv_i^2(t)+\tfrac{1}{2}\sum_{\vec{\nu}}\sum_{j\neq i}u[\,|\,\vec{r}_{ij}(t)-\vec{L}_{\vec{\nu}}\,|\,], \tag{3.12}$$

through the (caloric) equation of state $e(T,n)$. For small departures from the overall equilibrium state (e,n,T), we have

$$\delta T(\vec{r},t)=\left[\frac{\partial T}{\partial e}\right]_n\delta e(\vec{r},t)+\left[\frac{\partial T}{\partial n}\right]_e\delta n(\vec{r},t)+\cdots,$$
$$\delta T(\vec{r},t)=T(\vec{r},t)-T,$$
$$\delta e(\vec{r},t)=e(\vec{r},t)-e, \tag{3.13}$$
$$\delta n(\vec{r},t)=n(\vec{r},t)-n.$$

It should be observed that the hydrodynamic fields are periodic in $\vec{r}$, so that the local-equilibrium distribution functions are also periodic.

The significance of assumption I is discussed thoroughly by EHvL who regard it as the fundamental step in the theory. We do not recapitulate that discussion here. We replace $f^{(s)}$, then, by $f_l^{(s)}$ from Eq. (3.10) whence Eq. (3.8) becomes, after performing the velocity integration,

$$\langle v_{1x}(t)\rangle_n=\int_V d\vec{r}\,P(\vec{r},t)u_x(\vec{r},t) \tag{3.14}$$

which leads through Eq. (3.6) to the expression of the velocity-autocorrelation function as a product of two hydrodynamic fields.

We introduce now the second EHvL assumption: The long-wavelength components of $n(\vec{r},t)$, $\vec{u}(\vec{r},t)$, and $T(\vec{r},t)$ are governed by the equations of hydrodynamics, and $P(\vec{r},t)$ is similarly governed by Fick's law of self-diffusion. The reader is again referred to EHvL for a discussion of this assumption. The equations of hydrodynamics are written

$$\frac{\partial}{\partial t}n(\vec{r},t)=-n\vec{\nabla}\cdot\vec{u}(\vec{r},t),$$
$$\frac{\partial}{\partial t}\vec{u}(\vec{r},t)=-\frac{c^2}{\gamma n}\vec{\nabla}n(\vec{r},t)-\frac{\alpha c^2}{\gamma}\vec{\nabla}T(\vec{r},t)+\nu\nabla^2\vec{u}(\vec{r},t)+(D_l-\nu)\vec{\nabla}\vec{\nabla}\cdot\vec{u}(\vec{r},t), \tag{3.15}$$
$$\frac{\partial}{\partial t}T(\vec{r},t)=-\frac{\gamma-1}{\gamma}\vec{\nabla}\cdot\vec{u}(\vec{r},t)+\gamma D_T\nabla^2T(\vec{r},t),$$

where p is the pressure and

$$\alpha=-n^{-1}\left[\frac{\partial n}{\partial T}\right]_p,$$
$$\gamma=c_p/c_v, \tag{3.16}$$
$$c^2=m^{-1}\left[\frac{\partial p}{\partial n}\right]_s,$$

with c_p and c_v the heat capacities per particle at

constant pressure and volume, respectively, and with s the entropy per particle. Finally ν is the kinematic viscosity, D_T the thermal diffusivity, and D_l the longitudinal diffusivity, given by

$$\begin{aligned} \nu &= \eta/nm \ , \\ D_T &= \lambda/nc_p \ , \\ D_l &= \zeta/nm + 2(d-1)\nu/d \ , \end{aligned} \tag{3.17}$$

in terms of the coefficients of shear viscosity η, bulk viscosity ζ, and thermal conductivity λ. These equations are supplemented by Fick's law,

$$\frac{\partial}{\partial t} P(\vec{r},t) = D\nabla^2 P(\vec{r},t) \ , \tag{3.18}$$

where D is the self-diffusion constant.

C. Solution of hydrodynamic equations

Because the deviations from a uniform equilibrium state are assumed to be small, we linearize Eq. (3.15) in δn, $\vec{u}$, and δT. In addition, we define the Fourier series

$$\begin{aligned} h(\vec{r},t) &= V^{-1} \sum_{\vec{k}} h_{\vec{k}}(t) \exp(2\pi i \vec{k}\cdot\vec{r}/L) \ , \\ h_{\vec{k}}(t) &= \int_V d\vec{r}\, h(\vec{r},t) \exp(-2\pi i \vec{k}\cdot\vec{r}/L) \ , \end{aligned} \tag{3.19}$$

for an arbitrary function $h(\vec{r},t)$, where to simplify notation we have now taken the volume to be a d-dimensional cube[21] of edge L. Then Eqs. (3.15) and (3.18) become

$$\frac{d}{dt} \tilde{\underline{q}}_{\vec{k}}(t) = \tilde{\underline{M}}_{\vec{k}} \cdot \tilde{\underline{q}}_{\vec{k}}(t) \ , \tag{3.20a}$$

$$\frac{d}{dt} P_{\vec{k}}(t) = -\kappa^2 D P_{\vec{k}}(t) \ , \tag{3.20b}$$

where

$$\tilde{\underline{q}}_{\vec{k}}(t) = \begin{bmatrix} \delta n_{\vec{k}}(t) \\ \vec{u}_{\vec{k}}(t) \\ \delta T_{\vec{k}}(t) \end{bmatrix} \ , \qquad \vec{\kappa} = (2\pi/L)\vec{k} \ , \tag{3.21}$$

and where the coefficient matrix $\tilde{\underline{M}}_{\vec{k}}$ is given in the Appendix.

The solution of Eqs. (3.20) is, of course, standard (see e.g., EHvL) so that we omit most details. It is, however, a matter of some importance that we treat the $\vec{k}=0$ case separately. Using the fact that $\tilde{\underline{M}}_0 = 0$ (see the Appendix), Eq. (3.20) yields

$$\begin{aligned} \tilde{\underline{q}}_{\vec{0}}(t) &= \tilde{\underline{q}}_{\vec{0}}(0) \ , \\ P_{\vec{0}}(t) &= P_{\vec{0}}(0) \ , \end{aligned} \tag{3.22}$$

which is nothing more than the conservation laws. For nonvanishing $\vec{k}$, we let

$$\begin{aligned} \vec{u}^{\parallel}_{\vec{k}}(t) &= [\vec{u}_{\vec{k}}(t)\cdot\hat{k}]\hat{k} \ , \\ \vec{u}_{\vec{k}}(t) &= \vec{u}^{\parallel}_{\vec{k}}(t) + \vec{u}^{\perp}_{\vec{k}}(t) \ . \end{aligned} \tag{3.23}$$

One finds,

$$\frac{d}{dt} \vec{u}^{\perp}_{\vec{k}}(t) = -\nu\kappa^2 \vec{u}^{\perp}_{\vec{k}}(t) \ , \tag{3.24a}$$

$$\frac{d}{dt} \underline{q}_{\vec{k}}(t) = \kappa \underline{Q}_{\vec{k}} \cdot \underline{q}_{\vec{k}}(t) \ , \tag{3.24b}$$

where

$$\underline{q}_{\vec{k}}(t) = \begin{bmatrix} \delta n_{\vec{k}}(t) \\ u^{\parallel}_{\vec{k}}(t) \\ \delta T_{\vec{k}}(t) \end{bmatrix}$$

with the matrix $\underline{Q}_{\vec{k}}$ also given in the Appendix. Assuming the initial data $\underline{q}_{\vec{k}}(0)$ are known, we write the solution for the system of three equations in terms of the fundamental solution matrix $\underline{\Omega}_{\vec{k}}(t)$,

$$\begin{aligned} \underline{q}_{\vec{k}}(t) &= \underline{\Omega}_{\vec{k}}(t)\cdot\underline{\Omega}_{\vec{k}}(0)^{-1}\cdot\underline{q}_{\vec{k}}(0) \ , \\ \underline{\Omega}_{\vec{k}}(t) &= [\underline{w}_+ \exp(-\kappa\omega_+ t), \underline{w}_- \exp(-\kappa\omega_- t), \underline{w}_H \exp(-\kappa\omega_H t)] \ , \end{aligned} \tag{3.25}$$

where the $\underline{w}$ and ω are the eigenvectors and eigenvalues of $\underline{Q}_{\vec{k}}$,

$$\underline{Q}_{\vec{k}} \cdot \underline{w} = -\omega \underline{w}$$

and where subscripts H, $+$, and $-$ label the hydrodynamic modes, viz., the heat mode and the two sound modes.

The long-time behavior of the solutions Eq. (3.25) are dominated by the long-wavelength components. We simplify therefore by expanding the eigenvalues and eigenvectors in powers of κ,

$$\begin{aligned} \omega &= \omega^{(0)} + \kappa\omega^{(1)} + \cdots \ , \\ \underline{w} &= \underline{w}^{(0)} + \kappa\underline{w}^{(1)} + \cdots \ , \end{aligned}$$

and obtain to leading order in κ:

$$\begin{aligned}
\delta n_{\vec{k}}(t) &= nc^{-1}[A^{+}_{\vec{k}}\exp(-\kappa\omega_{+}t) \\
&\quad + A^{-}_{\vec{k}}\exp(-\kappa\omega_{-}t)] \\
&\quad + A^{H}_{\vec{k}}\exp(-\kappa\omega_{H}t) , \\
u^{\parallel}_{\vec{k}}(t) &= A^{+}_{\vec{k}}\exp(-\kappa\omega_{+}t) - A^{-}_{\vec{k}}\exp(-\kappa\omega_{-}t) , \\
\delta T_{\vec{k}}(t) &= T^{s}_{\vec{k}}(t) + T^{H}_{\vec{k}}(t) , \\
T^{s}_{\vec{k}}(t) &= [(\gamma-1)/\alpha c] \\
&\quad \times [A^{+}_{\vec{k}}\exp(-\kappa\omega_{+}t) \\
&\quad + A^{-}_{\vec{k}}\exp(-\kappa\omega_{-}t)] , \\
T^{H}_{\vec{k}}(t) &= -(1/\alpha n)A^{H}_{\vec{k}}\exp(-\kappa\omega_{H}t) ,
\end{aligned} \tag{3.26}$$

where

$$\begin{aligned}
A^{\pm}_{\vec{k}} &= (c/2\gamma n)[\delta n_{\vec{k}}(0) + n\alpha\delta T_{\vec{k}}(0)] \\
&\quad \pm \tfrac{1}{2}u^{\parallel}_{\vec{k}}(0) , \\
A^{H}_{\vec{k}} &= [(\gamma-1)/\gamma]\delta n_{\vec{k}}(0) - (\alpha n/\gamma)\delta T_{\vec{k}}(0) .
\end{aligned}$$

The leading terms in the eigenvalues are

$$\begin{aligned}
\omega_{\pm} &= \pm ic + \kappa\Gamma_s/2 + \cdots , \\
\omega_{H} &= \kappa D_T + \cdots ,
\end{aligned} \tag{3.27}$$

where $\Gamma_s = D_l + (\gamma-1)D_T$ is the acoustic attenuation coefficient.

The solution is completed by integrating the uncoupled Eqs. (3.20b) and (3.24a), yielding

$$\begin{aligned}
P_{\vec{k}}(t) &= P_{\vec{k}}(0)\exp(-\kappa^2 Dt) , \\
\vec{u}^{\perp}_{\vec{k}}(t) &= \vec{u}^{\perp}_{\vec{k}}(0)\exp(-\kappa^2\nu t) .
\end{aligned} \tag{3.28}$$

Equations (3.22), (3.26), and (3.28) complete the hydrodynamic solution for the $d+2$ hydrodynamic fields in terms of the initial values for the latter.

D. Initial hydrodynamic fields

The determination of the initial data $n_{\vec{k}}(0)$, $u_{\vec{k}}(0)$, $T_{\vec{k}}(0)$, and $P_{\vec{k}}(0)$ is not a simple matter. While it may be true, as asserted by assumptions I and II, that $n_{\vec{k}}(t)$, for example, evolves according to the hydrodynamic equations after a few mean-free times, the exact $n_{\vec{k}}(t)$ and its hydrodynamic value are expected to disagree when followed backward to $t=0$. Only the $\vec{k}=0$ components of the exact $n(\vec{r},t)$, $\vec{u}(\vec{r},t)$, $e(\vec{r},t)$, and $P(\vec{r},t)$ and the hydrodynamic fields agree for all times, by virtue of the conservation of mass, momentum, energy, and number of tagged particles.

For the EHvL theory, only the long-wavelength specification was needed, because the theory was only concerned with the asymptotic time dependence. Here we are somewhat more ambitious, hoping to find the correlation functions at times which are long only in this sense that the hydrodynamic regime has been established. This involves, as we shall see, wavelengths which are not infinite, but which are of the order of the cell edge L. The only available approximations for $n_{\vec{k}}(0)$, $\vec{u}_{\vec{k}}(0)$, $T_{\vec{k}}(0)$, and $P_{\vec{k}}(0)$ are the nonequilibrium ensemble values. We shall use these, then, and understand that the theory should hold, provided the system length L is not too small.

We compute first the number density. From Eqs. (3.3), (3.5), and (3.11a) we obtain

$$\begin{aligned}
\delta n(\vec{r},0) &= W(\vec{r}-\vec{r}_0) \\
&\quad + n\int_V d\vec{r}\,' W(\vec{r}\,'-\vec{r}_0)G_N(\vec{r}-\vec{r}\,') , \\
G_N(\vec{r}-\vec{r}\,') &= g_N(\vec{r}-\vec{r}\,') - 1 ,
\end{aligned} \tag{3.29}$$

$$\delta n_{\vec{k}}(0) = W_{\vec{k}}(1 + nG_{N\vec{k}})\exp(-i\vec{\kappa}\cdot\vec{r}_0) ,$$

where $g_N(\vec{r})$ is the pair-correlation function. We observe that in the $\vec{k}\to 0$ limit, $G_{N\vec{k}}\to -1/n$ so that $\delta n_{\vec{0}}=0$, which differs from the grand-canonical-ensemble result of EHvL. As we shall see below, this difference does not affect $\rho_D(t)$.

In similar fashion, for the velocity field we obtain from Eqs. (3.3), (3.5), and (3.11b)

$$\begin{aligned}
n(\vec{r},0)\vec{u}(\vec{r},0) &= \vec{v}_0 W(\vec{r}-\vec{r}_0) , \\
\vec{u}_{\vec{k}}(0) &= \vec{v}_0(W_{\vec{k}}/n)\exp(-i\vec{\kappa}\cdot\vec{r}_0) ,
\end{aligned} \tag{3.30}$$

where second-order terms in the fluctuations have been ignored. For the internal energy we obtain from Eqs. (3.3), (3.5), and (3.12)

$$\begin{aligned}
\delta e(\vec{r},0) &= (mv_0^2/2 - d/2\beta)W(\vec{r}-\vec{r}_0) \\
&\quad + n^{-1}\int_V d\vec{r}\,' W(\vec{r}\,'-\vec{r}_0)G^{(e)}_N(\vec{r}\,'-\vec{r}) , \\
G^{(e)}_N(\vec{r}) &= g^{(e)}_N(\vec{r}) - ne , \\
g^{(e)}_N(\vec{r}-\vec{r}\,') &= \left\langle \sum_{i=1}^{N}\delta(\vec{r}_i-\vec{r}) \sum_{j=1}^{N}\delta(\vec{r}_j-\vec{r}\,')e_j \right\rangle , \\
\delta e_{\vec{k}}(0) &= W_{\vec{k}}(mv_0^2/2 - d/2\beta + n^{-1}G^{(e)}_{N\vec{k}}) \\
&\quad \times \exp(-i\vec{\kappa}\cdot\vec{r}_0) .
\end{aligned} \tag{3.31}$$

In the canonical ensemble $G^{(e)}_{N\vec{k}}$ vanishes as $\vec{k}\to 0$, whence

$$\delta e_{\vec{0}}(0)=\tfrac{1}{2}mv_0^2-d/2\beta$$

which again contrasts with the EHvL result for the grand canonical ensemble.

Because we require the initial temperature field in Eq. (3.26) rather than $e(\vec{r},0)$, we use Eq. (3.13) with

$$\left[\frac{\partial T}{\partial e}\right]_n=\frac{1}{nc_v}\,,$$

$$\left[\frac{\partial T}{\partial n}\right]_e=\frac{\gamma-1}{n\alpha}-\frac{p+e}{n^2c_v}\,,$$

to obtain, using Eq. (3.31),

$$\delta T_{\vec{k}}(0)=\left[\frac{1}{nc_v}(mv_0^2/2-d/2\beta+n^{-1}G^{(e)}_{N\vec{k}})-\frac{p+e}{n^2c_v}(1+nG_{N\vec{k}})\right]W_{\vec{k}}\times\exp(-i\vec{\kappa}\cdot\vec{r}_0)\,. \tag{3.32}$$

Finally for the tagged-particle density we have from Eqs. (3.3), (3.5), and (3.11c),

$$P(\vec{r},0)=W(\vec{r}-\vec{r}_0)\,,\qquad P_{\vec{k}}(0)=W_{\vec{k}}\exp(-i\kappa\cdot\vec{r}_0)\,. \tag{3.33}$$

E. Velocity-autocorrelation function

We compute the velocity-autocorrelation function from Eqs. (3.6) and (3.14), writing $P(\vec{r},t)$ and $\vec{u}(\vec{r},t)$ as Fourier sums of the form of Eq. (3.19) and with $\vec{u}_{\vec{k}}(t)$ given as the sum of $u^{\parallel}_{\vec{k}}$ and $\vec{u}^{\perp}_{\vec{k}}$ as in Eq. (3.23), for $\vec{k}\neq 0$. For $\vec{k}=0$, because $\vec{u}_{\vec{0}}(t)$ is, from Eqs. (3.21) and (3.22), independent of the time, we can simply *define* a convenient similar separation of $\vec{u}_0(t)$ to be

$$\vec{u}^{\perp}_{\vec{0}}(t)=\vec{u}_{\vec{0}}(0)-\vec{u}^{\parallel}_{\vec{0}}(0)\,,$$

$$u^{\parallel}_{\vec{0}}(t)=[\vec{u}_{\vec{0}}(0)\cdot\hat{e}_1]\hat{e}_1\,,$$

whence Eqs. (3.26) and (3.28) apply for all $\vec{k}$. We may then write

$$c_D(t)=c_D^{\perp}(t)+c_D^{\parallel}(t)\,, \tag{3.34}$$

$$c_D^{l}=(dV)^{-1}\int_V d\vec{r}_0\int d\vec{v}_0\varphi_0(v_0)V^{-1}\times\sum_{\vec{k}}P_{-\vec{k}}(t)\vec{u}^{l}_{\vec{k}}(t)\cdot\vec{v}_0\,,$$

for $l=\perp$ or $\parallel$. We substitute $P_{\vec{k}}(t)$ from Eq. (3.28) and $\vec{u}_{\vec{k}}(t)$ from Eqs. (3.26) and (3.28) into the second equation of (3.34) to obtain

$$c_D^{\perp}(t)=[(d-1)/dn\beta mV]\sum_{\vec{k}}W_{\vec{k}}W_{-\vec{k}}\exp[-\kappa^2(D+\nu)t]\,,$$

$$c_D^{\parallel}(t)=(1/dn\beta mV)\sum_{\vec{k}}W_{\vec{k}}W_{-\vec{k}}\cos(c\kappa t)\exp[-\kappa^2(D+\Gamma_s/2)t]\,. \tag{3.35}$$

The so-called shear-mode term $c_D^{\perp}$ is essentially the one discussed by Keyes and Ladanyi[20] and in the thermodynamic limit it is dominant at long times, leading to the long-time tail equation (1.1). The acoustic-mode term $c_D^{\parallel}$ will be shown to have considerable importance for the finite systems of particular interest here. It is of interest to observe that in the long-time limit the $\vec{k}=0$ terms dominate Eq. (3.35), whence $c_D(t)\to 1/N\beta m$, and from Eq. (2.5), $\rho_D(t)\to 0$.

The initial distribution $W(\vec{r})$ of the tagged particle is seen to enter into our final result in an important way, even though in the derivation its properties do not enter. It would have seemed natural at the outset to use a δ-function initial distribution for the position as well as the velocity of the tagged particle. Nonetheless, to study the effect of this distribution, we assume $W(\vec{r})$ to have the form of a Gaussian of sufficiently narrow width that we can ignore the finite size of the volume V in computing its normalization and its Fourier components. We take

$$W(\vec{r})=[(2\pi)^{1/2}\mu]^{-d}\exp(-r^2/2\mu^2)\,,\qquad W_{\vec{k}}=\exp(\kappa^2\mu^2/2)\,, \tag{3.36}$$

where μ is a parameter measuring the width of the distribution. From Eq. (3.35) then, we see that the effect of the width of $W(\vec{r})$ is to redefine the origin of the time for $c_D^{\perp}$, but is more complicated for $c_D^{\parallel}$.

F. Limiting form of VACF for large systems

It is of particular interest to study the approach of the result, Eq. (3.35), to the infinite-system limit.

A form of these functions which is particularly useful in this regard can be obtained by using the d-dimensional Poisson-sum formula[22]

$$L^{-d}\sum_{\vec{k}} h(k/L) = \sum_{\vec{l}} \int d\vec{r}\, h(r)\exp(-2\pi i \vec{r}\cdot\vec{l}L) \quad (3.37)$$

for an arbitrary function $h(k/L)$, in which the $\vec{r}$ integration extends over infinite d-dimensional space. We note at the outset that the $\vec{l}=0$ term on the right yields for $c_D^{\perp}(t)$ the thermodynamic $c_{D\infty}^{\perp}(t)$. Indeed, one obtains from Eqs. (3.35), (3.36), and (3.37),

$$\begin{aligned} c_D^{\perp}(t) &= c_{D\infty}^{\perp}(t)+\Delta c_D^{\perp}(t)\ , \\ c_{D\infty}^{\perp} &= [(d-1)/dn\beta m] \\ &\quad\times\{4\pi[\mu^2+(D+\nu)t]\}^{-d/2}\ , \\ \Delta c_D^{\perp} &= c_{D\infty}^{\perp}(t) \\ &\quad\times\sum_{\vec{l}}{}'\exp\left[-\frac{l^2L^2}{4[\mu^2+(D+\nu)t]}\right], \end{aligned} \quad (3.38)$$

where the prime on the $\vec{l}$ sum indicates the absence of the $\vec{l}=0$ term. The corrections to the infinite-system limit $c_{D\infty}^{\perp}(t)$ are seen, then, to decay exponentially with the square of the length of the system. Moreover, we note that $c_{D\infty}^{\perp}(t)$ reduces to Eq. (1.1) for a δ function for $W(\vec{r})$, i.e., for $\mu=0$.

For the acoustic-mode component, one similarly obtains

$$\begin{aligned} c_D^{\parallel}(t) &= c_{D\infty}^{\parallel}(t)+\Delta c_D^{\parallel}(t)\ , \\ c_{D\infty}^{\parallel} &= (1/dn\beta m) \\ &\quad\times\{4\pi[\mu^2+(D+\Gamma_s/2)t]\}^{-d/2} \\ &\quad\times {}_1F_1[d/2,\tfrac{1}{2},\beta_D(t)]\ , \\ \beta_D(t) &= \frac{c^2t^2}{4[\mu^2+(D+\Gamma_s/2)t]}\ , \end{aligned} \quad (3.39)$$

in which the leading ($\vec{l}=0$) term has been evaluated[23] in terms of the confluent hypergeometric function ${}_1F_1$. For the three-dimensional case, one can write this result in terms of elementary functions by evaluating the $\vec{r}$ integral in Eq. (3.37) for arbitrary $\vec{l}$ to obtain

$$\begin{aligned} c_{D\infty}^{\parallel}(t) &= \gamma_D(t)[1-2\beta_D(t)] \\ &\quad\times\exp[-\beta_D(t)] \quad (\text{for } d=3) \\ \Delta c_D^{\parallel}(t) &= \tfrac{1}{2}\gamma_D(t)\sum_{\vec{l}}{}'\left[e_l^{+}(t)+e_l^{-}(t)\right. \\ &\quad\left.+\frac{ct}{lL}[e_l^{+}(t)-e_l^{-}(t)]\right], \\ \gamma_D(t) &= \{4\pi dn\,\beta m[\mu^2+(D+\Gamma_s/2)t]^{3/2}\}^{-1}\ , \\ e_l^{\pm} &= \exp\left[-\frac{(lL\pm ct)^2}{4[\mu^2+(D+\nu)t]}\right], \end{aligned} \quad (3.40)$$

which can be shown to agree with Eq. (3.39) for $c_{D\infty}^{\parallel}(t)$. This result will be used in a subsequent paper on hard-sphere results. Again we note the exponential decay with L^2 of the finite-system correction terms.

For the two-dimensional case, we have been unable to completely evaluate the same $\vec{r}$ integral in Eq. (3.37) and have not obtained a convenient expression for $\Delta c_D^{\parallel}(t)$. [This does not prevent one, of course, from using Eq. (3.35) for evaluating $c_D^{\parallel}(t)$ numerically.]

In the numerical evaluation of the theoretical $c_D(t)$, we use the sums Eqs. (3.35) for values of the time sufficiently large that these converge rapidly. For $d=3$ we use Eq. (3.40) for smaller values of the time. For $d=2$ we continue to use Eq. (3.35) even for rather small values of the time, or if convergence is impractically slow, we use $c_{D\infty}^{\parallel}(t)$ from Eq. (3.39), using the infinite series to evaluate the latter.[23]

The question of what values for the transport coefficients should be used in the theoretical formulas was discussed by EHvL, both for $d=3$ for which the transport coefficients exist, and for $d=2$ for which the macroscopic transport coefficients are infinite. We[11] have also discussed this question with regard to the time-correlation functions for shear viscosity for hard spheres. In two dimensions we will normally use the Enskog values, although it might be more consistent to use the MD values defined as the integral of the appropriate time-correlation function for the finite system,[24] or even values defined as the integral out to the current value of the time [see, for example, Eq. (2.3b) for $D(t)$].

G. VACF in microcanonical ensemble

While the VACF has been calculated in this section for the canonical ensemble, our numerical re-

sults are microcanonical ensemble estimates. The differences between the two ensembles is, of course, expected to be of order $1/N$.

To relate the two, we consider the ensemble average for an arbitrary phase function in the microcanonical ensemble

$$\langle f(\underline{x}^N)\rangle_{NVE}=Z_{NVE}^{-1}\int_V d\underline{r}^N\int d\underline{v}^N A(\underline{r}^N)\delta(E-mv^2/2)f(\underline{x}^N)\ , \tag{3.41}$$

where $A(\underline{r}^N)$ is the overlap function [viz., $A(\underline{r}^N)$ vanishes if any r_{ij} is less than σ and is unity elsewhere], v is the magnitude of $\underline{v}^N$, and where Z_{NVE} is the partition function

$$Z_{NVE}=\int_V d\underline{r}^N\int d\underline{v}^N A(\underline{r}^N)\delta(E-mv^2/2)\ . \tag{3.42}$$

The velocity integral in Eq. (3.42) can be evaluated in terms of the Γ function, whence

$$Z_{NVE}=\frac{\pi^{Nd/2}dN}{\Gamma(1+Nd/2)m}\left[\frac{2E}{m}\right]^{Nd/2-1}Q_{NV}\ ,\quad Q_{NV}=\int d\underline{r}^N A(\underline{r}^N)\ . \tag{3.43}$$

In similar fashion, the NVT-ensemble average is

$$\langle f(\underline{x}^N)\rangle_{NVT}=Z_{NVT}^{-1}\int_V d\underline{r}^N\int d\underline{v}^N A(\underline{r}^N)\exp(-\beta mv^2/2)f(\underline{x}^N)\ , \tag{3.44}$$

where the canonical-ensemble partition function is

$$Z_{NVT}=\int_V d\underline{r}^N\int d\underline{v}^N A(\underline{r}^N)\exp(-\beta mv^2/2)=\left[\frac{2\pi}{m\beta}\right]^{Nd/2}Q_{NV}\ . \tag{3.45}$$

By introducing a factor $\delta(E-mV^2/2)$ together with an additional energy integration on the right of Eq. (3.44), and using Eqs. (3.43) and (3.45), one obtains

$$\langle f(\underline{x}^N)\rangle_{NVT}=\frac{Nd}{2\Gamma(1+Nd/2)}\int_0^\infty d(\beta E)\exp(-\beta E)(\beta E)^{Nd/2-1}\langle f(\underline{x}^N)\rangle_{NVE}\ . \tag{3.46}$$

To apply this to the velocity-autocorrelation function, we require the energy dependence of the latter. For this purpose, we use the scaling of the time dependence of the trajectory with the magnitude of the velocity. If we let $\underline{r}^N(t;\underline{r}^N,\underline{v}^N)$ and $\underline{v}^N(t;\underline{r}^N,\underline{v}^N)$ denote the trajectory through the initial point $\underline{r}^N,\underline{v}^N$, then for any factor α,

$$\underline{r}^N(t;\underline{r}^N,\alpha\underline{v}^N)=\underline{r}^N(\alpha t;\underline{r}^N,\underline{v}^N),\quad \underline{v}^N(t;\underline{r}^N,\alpha\underline{v}^N)=\alpha\underline{v}^N(\alpha t;\underline{r}^N,\underline{v}^N)\ .$$

Thus

$$\langle v_{1x}(0)v_{1x}(t)\rangle_{NVE}=\frac{E}{E_0}\langle v_{1x}(0)v_{1x}[t(E/E_0)^{1/2}]\rangle_{NVE_0}\ . \tag{3.47}$$

Now for large N, it is anticipated that the principal contribution to the integral Eq. (3.46) will arise for $E\approx Nd/2\beta$ for which the factor $(\beta m)^{Nd/2}\exp(-\beta E)$ has its maximum. Therefore we substitute Eq. (3.47) with $E_0=Nd/2\beta$ into Eq. (3.46) to obtain

$$\begin{aligned}&\langle v_{1x}(0)v_{1x}(t)\rangle_{NVT}=\frac{2\xi^{\xi+1}}{\Gamma(\xi+1)}\mathscr{I}(\xi)\ ,\\ &\mathscr{I}(\xi)=\int_0^\infty d\alpha\,\alpha\exp[\xi h(\alpha)]\langle v_{1x}(0)v_{1x}(\alpha t)\rangle_{NVE_0}\ ,\end{aligned} \tag{3.48}$$

in which $\xi=\beta E_0=Nd/2$, $\alpha=(\beta E/\xi)^{1/2}$, and $h(\alpha)=-\alpha^2+2\ln\alpha$. One can evaluate $\mathscr{I}(\xi)$ for large ξ as a series of inverse powers by expanding the integrand about $\alpha=1$. One obtains

$$\mathscr{I}(\xi)=e^{-\xi}\left[\frac{\pi}{2\xi}\right]^{1/2}\left[1+\frac{1}{2\xi}\left[\frac{1}{6}+\frac{3}{4}t\frac{d}{dt}+\frac{1}{4}t^2\frac{d^2}{dt^2}\right]+O(\xi^{-3/2})\right]\langle v_{1x}(0)v_{1x}(t)\rangle_{NVE_0}\ . \tag{3.49}$$

Combining Eq. (3.49) and the expansion of the Γ function with Eq. (3.48), we obtain

$$\langle v_{1x}(0)v_{1x}(t)\rangle_{NVT}=\left[1+\frac{1}{4Nd}\left[3t\frac{d}{dt}+t^2\frac{d^2}{dt^2}\right]+O(1/N^2)\right]\langle v_{1x}(0)v_{1x}(t)\rangle_{NVE_0}\,, \tag{3.50}$$

or solving for the microcanonical ensemble average,

$$\langle v_{1x}(0)v_{1x}(t)\rangle_{NVE_0}=\left[1-\frac{1}{4Nd}\left[3t\frac{d}{dt}+t^2\frac{d^2}{dt^2}\right]+O(1/N^2)\right]\langle v_{1x}(0)v_{1x}(t)\rangle_{NVT}\,. \tag{3.51}$$

Used with Eq. (3.35), one obtains the EHvL result for the NVE ensemble to order $1/N^2$.

IV. MONTE CARLO MOLECULAR-DYNAMICS METHOD

Our numerical estimates of the velocity-autocorrelation function are based on a combined Monte Carlo and molecular-dynamics method which has been described in some detail elsewhere.[10] Briefly, we estimate the $\rho_D(t)$ as averages over P dynamical trajectories $\{\underline{x}_p^N(t);p=1,2,\ldots,P\}$,

$$\rho_D(t)=P^{-1}\sum_{p=1}^{P}\rho_{D_p}(t)\,, \tag{4.1}$$

where $\rho_{D_p}(t)$ is the estimate for the VACF for trajectory p. For each trajectory, the particle positions $\underline{r}_p^N(0)$ at the initial time $t=0$ are sampled by ordinary Metropolis MC techniques[25] from a statistical mechanical ensemble. Typically a move attempt is made for each particle sequentially, with several tens of attempts to move each particle being made in proceeding from the initial configuration $\underline{r}_p^N(0)$ to initial configuration $\underline{r}_{p+1}^N(0)$ for the next trajectory. Thus, successive points $\underline{r}_p^N(0)$ and $\underline{r}_{p+1}^N(0)$ are not strongly correlated. The initial velocities $\underline{v}_p^N(0)$ are selected by independent trials by a method dependent on the ensemble. For the canonical ensemble, for example, the velocities are sampled from the Maxwell-Boltzmann distribution by the Box-Muller method.[26] For the microcanonical ensemble (which should be distinguished from the "molecular-dynamics" ensemble for which $\vec{P}=0$), we simply scale the canonical-ensemble velocities to yield the fixed energy E.

The current version of the program computes the velocity-autocorrelation function at observation times which are of variable spacing, viz., at times $t=k_1h,\ 2k_1h,\ldots,n_1k_1h,\ (n_1k_1+k_2)h,\ (n_1k_1+2k_2)h,\ldots,(n_1k_1+n_2k_2)h,\ldots,Mh$, where the n_i and k_i are integers, with $M=\sum n_ik_i$, and where h is a time step, specified in units of the mean-free time given by the low-density, finite-system expression

$$t_{00}^{(N)}=\frac{V}{(N-1)(2\sigma)^{d-1}}\left[\frac{m\beta}{\pi}\right]^{1/2}. \tag{4.2}$$

For the most part, however, the data were obtained from an earlier version of the program for which the spacing of observation times is uniform, viz., $\{n_i\}=\{M\}$ and $\{k_i\}=\{1\}$. Each trajectory is generated to a fixed number θ of time steps with $\theta\geq M$. On each trajectory the $\rho_D(t)$ are time averaged by defining the phases $\underline{x}^N(t)$ at times $t=0,\ \omega h,\ 2\omega h,\ldots,\Omega h$ (ω and Ω integers) as "time origins." Then the time average on trajectory p is given by the average over time origins

$$\rho_{D_p}(t)=\frac{1}{(J+1)Nd}\times\sum_{j=0}^{J}\sum_{i=1}^{N}\vec{u}_{i_p}(j\omega h)\cdot\vec{u}_{i_p}(t+j\omega h)\,, \tag{4.3}$$

$$J=I\left[\frac{\theta h-t}{\omega h}\right],$$

in which $I(x)$ is the integer part of x. In practice, the spacing of time origins is a matter of considerable importance in determining the statistical uncertainty of the VACF. We have typically used values of ω such that time origins are from 1 to 10 mean-free times apart; more closely spaced values yield contributions to the j sum in Eq. (4.3) which are excessively correlated. The more widely spaced values appear to be inefficient use of computer time.

It is of interest to observe that the calculation of the VACF, Eq. (4.3), was performed physically at the same time the trajectory was generated on the computer. As a result, in many instances choices of time-step and time-origin spacing were less than optimal but could not be modified without rerunning a very long (in computer time) calculation. This situation contrasts to the typical practice for MD calculations for soft potentials in which the trajectory is recorded (e.g., on magnetic tape), with the calcu-

lation of phase functions then performed later, using the recorded trajectory. For hard spheres and disks, a detailed record of the trajectory (e.g., consisting of the phases of the colliding pair of particles after each collision) would be too voluminous for currently available secondary storage devices. However, after virtually all the current results were obtained, we devised a means of compactly recording a trajectory by simply saving the identity of the pair of particles involved in each collision, in addition to the initial phase of the system. From this information one can regenerate the trajectory exactly, without the need to perform the time-consuming step of determining the next collision.

While nearly all the calculations reported here generate averages as described above, we have found empirically that the sampling of initial velocities for the particles is not generally adequate when the usual pseudorandom-number generators[26] are used in the Box-Muller method. This is reflected, for example, in the initial behavior of the VACF, for realizations (not reported here) in which no time averaging is used, i.e., $J=0$ in Eq. (4.3). The results reported here do not reflect the problem because of the use of extensive time averaging and because of the fact that the undesirable correlations present in the initial velocities decay rapidly with time. Therefore, a better procedure for the sampling of initial phases is realized when one adds a "thermalization" step in which the initial phase is taken to be the actual phase generated after some fixed time on the current trajectory. Such a thermalization process is, of course, normally used in molecular-dynamics calculations which involve a single long trajectory.

In addition to the observation of $\rho_D(t)$ directly from Eqs. (4.1) and (4.3), it is of interest to compute the time-dependent self-diffusion constant $D(t)$, Eq. (2.3b), which can be written, in view of Eq. (2.3c), as

$$D(t)=\langle u_{1x}(0)\Delta x_1(t)\rangle \ , \tag{4.4}$$

where $\Delta\vec{r}_i(t)$ denotes the displacement in the center-of-mass frame of reference

$$\Delta\vec{r}_i(t)=\vec{r}_i(t)-\vec{r}_i(0)-\vec{P}t/(Nm)$$

and $\Delta x_i(t)$ denotes the x component of $\Delta\vec{r}_i(t)$. Also of interest is the related quantity

$$D^{(f)}(t)=\langle u_{1x}(t)\Delta x_1(t)\rangle \tag{4.5}$$

for which it can be shown, using Liouville's theorem and the dynamic reversibility of the trajectory, that

$$D^{(f)}(t)=D(t) \ . \tag{4.6}$$

While Eq. (4.6) holds for the ensemble averages involved, it does not hold generally for the MCMD estimates of these quantities. Finally, we compute the mean-square displacement $\langle \Delta x_1^2(t)\rangle$ and the Einstein function

$$S(t)=\langle \Delta x_1^2(t)\rangle /2t \ . \tag{4.7}$$

Evidently,

$$D^{(f)}(t)=\frac{d}{dt}tS(t) \ . \tag{4.8}$$

The four quantities $\rho_D(t)$, $D(t)$, $D^{(f)}(t)$, and $S(t)$ are then all simply related. Numerical estimates for any one of them can be used to estimate the others through numerical differentiation or integration. One question we shall address is the relative merits of these various procedures for obtaining $\rho_D(t)$.

We report here time-correlation functions for hard-core systems scaled with respect to the Enskog self-diffusion constant

$$D_E=b_D^{(d)}D_{00}/\chi \ , \tag{4.9}$$

where D_{00} is the Boltzmann self-diffusion constant in the so-called first Enskog approximation

$$\begin{aligned} D_{00}&=\frac{dt_{00}}{2\beta m} \ , \\ t_{00}&=\frac{V}{N(2\sigma)^{d-1}}\left[\frac{m\beta}{\pi}\right]^{1/2} \ . \end{aligned} \tag{4.10}$$

χ is the pair-correlation function at contact, t_{00} is the Boltzmann mean-free time, and

$$\begin{aligned} b_D^{(2)}&=1.027\,09 \ , \\ b_D^{(3)}&=1.018\,96 \ , \end{aligned} \tag{4.11}$$

are the higher Sonine polynomial corrections in the Boltzmann theory, the hard-sphere value being that of Pekeris[27] and the hard-disk value being obtained by the method given by Chapman and Cowling[28] to the "ninth approximation." In particular, we define the reduced time-correlation functions

$$\begin{aligned} \bar{\rho}_D(s)&=t_0\rho_D(st_0)/D_E \ , \\ \bar{D}(s)&=\int_0^s ds'\bar{p}_D(s')=D(st_0)/D_E \ , \\ \bar{D}^{(f)}(s)&=D^{(f)}(st_0)/D_E \ , \\ \bar{S}(s)&=s^{-1}\int_0^s ds'\bar{D}^{(f)}(s')=S(st_0)/D_E \ , \end{aligned} \tag{4.12}$$

where s is the time in units of the mean-free time.

In order to reduce our data as in Eq. (4.12), we require χ, which we compute from the Padé (3×3)

approximant to the virial equation of state of Ree and Hoover,[29]

$$\varphi = pV_0/Nk_BT = (1+bn\chi)/\tau ,$$
$$\chi = A(1/\tau)/B(1/\tau) , \tag{4.13}$$
$$\tau = V/V_0 ,$$

where V_0 is the closed-packed volume $(3/2d)^{1/2}N\sigma^d$, with b the second virial coefficient

$$bn = \frac{(2/3d)^{1/2}\pi^{d/2}}{\Gamma(d/2)\tau} ,$$

$\Gamma(x)$ is the gamma function, and

$$A(x) = 1 + a_1^{(d)}x + a_2^{(d)}x^2 ,$$
$$B(x) = 1 + b_1^{(d)}x + b_2^{(d)}x^2 , \tag{4.14}$$

with the $a_i^{(d)}$ and $b_i^{(d)}$ given in Ref. 25. For the mean-free time which also appears in Eq. (4.12), we use the observed value for the particular MCMD realization under study.

In order to evaluate the theoretical VACF given by Eqs. (3.35)–(3.40) for comparison with the MCMD results, we require the transport coefficients D, η, ζ, and λ. For the most part we use the Enskog-theory values[28,30]

$$\eta_E = \frac{\eta_{00}}{\chi}\left[c_\eta^{(d)}\left[1+\frac{2}{d+2}bn\chi\right]^2 + \frac{16d}{(d+2)^2\pi}(bn\chi)^2\right] ,$$
$$\eta_{00} = (d+2)nmD_{00}/2d ,$$
$$c_\eta^{(2)} = 1.022 ,$$
$$c_\eta^{(3)} = 1.016 ,$$

$$\zeta_E = \frac{16}{(d+2)\pi}\frac{\eta_{00}}{\chi}(bn\chi)^2 , \tag{4.15}$$

$$\lambda_E = \frac{\lambda_{00}}{\chi}\left[c_\lambda^{(d)}\left[1+\frac{3}{d+2}bn\chi\right]^2 + \frac{16(d-1)}{(d+2)^2\pi}(bn\chi)^2\right] ,$$
$$\lambda_{00} = (d+2)^2nk_BD_{00}/2^d ,$$
$$c_\lambda^{(2)} = 1.029 ,$$
$$c_\lambda^{(3)} = 1.025\,13 ,$$

with D_E and D_{00} given in Eqs. (4.9) and (4.10). As we previously indicated, the time unit for our results is chosen to be the mean-free time t_0, for which we use the values observed in our MD calculations.

V. NUMERICAL ANALYSIS

In this section we report data for $\bar{\rho}_D(s)$ and compare them with the predictions of the mode-coupling theory at long times. Here we consider several preliminary questions concerning the method of evaluation of $\bar{\rho}_D(s)$ and the statistical analysis of the data.

A. Method of evaluation of VACF

In order to decide the relative merits of computing the VACF directly via Eq. (4.3), or from one of the related functions introduced in Sec. IV, we consider the specific case of a system of 5822 hard disks at a volume of $2V_0$ (where V_0 is the close-packed volume), for which 50 trajectories, each consisting of 120 time steps of length $h = 1.5t_{00}^{(N)} \approx 4.01t_0$, were generated with initial phase sampled from the microcanonical ensemble. The time-correlation functions $\bar{\rho}_D(s)$, $\bar{D}(s)$, $\bar{D}^{(f)}(s)$, and $\bar{S}(s)$ were computed at each time step out to $s = 80h$, with time origins defined at every second time step (i.e., $\omega = 2$).

To estimate $\bar{\rho}_D(s)$ from $\bar{D}(s)$, $\bar{D}^{(f)}(s)$, and $\bar{S}(s)$, we approximate the appropriate derivative with respect to the time by central differences. This, of course, introduces a systematic error associated with the higher differences which are ignored. The magnitude of this error can be estimated for long times by computing the first neglected term from the mode-coupling theory. For the results presented here, we conclude that the systematic error is small compared to the statistical uncertainty at least for $t > 20t_0$.

An additional factor which needs to be recognized in using numerical differences is that the smoothness of $\bar{D}(s)$, $\bar{D}^{(f)}(s)$, and $\bar{S}(s)$ with time is affected by the spacing ωh of time origins. For the 5822-particle system under consideration, $\bar{D}^{(f)}(s)$ and $\bar{S}(s)$ are found to have a slightly jumpy behavior at values of $s > 20$, with the values at time origins being relatively larger than those between time origins.[31] If one ignores values between time origins (or considers values located similarly with respect to time origins, e.g., one time step after each time origin), the jumpiness is largely removed. Therefore the three estimates $\bar{D}(s)'$, $\bar{D}^{(f)}(s)'$, and $[s\bar{S}(s)]''$ (the prime denoting a derivative with

respect to s) will depend on the differencing interval $\Delta t = kh$ used to estimate the derivatives. We denote these estimates through a leading subscript k, e.g., ${}_k\bar{D}(s)'$. In Fig. 1 then we plot seven estimates of the velocity-autocorrelation function, using values of both 1 and 2 for k, at selected values of the time. Evidently, the $k=1$ estimates from $\bar{D}^{(f)}(s)$ and $\bar{S}(s)$, involving differencing between a time origin and an adjacent point which is not a time origin, have large statistical uncertainties. The remaining estimates all have smaller statistical uncertainties than have the directly computed $\bar{\rho}_D(s)$, with ${}_2[s\bar{S}(s)]''$ having a standard deviation which is roughly half that of $\bar{\rho}_D(s)$.

For this particular system, therefore, ${}_\omega[s\bar{S}(s)]''$ provides the best estimate for $\bar{\rho}_D(s)$ at long times. It turns out, in fact, that the same conclusion holds for essentially all system parameters used in these calculations. At smaller values of s, however, the systematic errors tend to be larger and we have normally used the directly computed $\bar{\rho}_D(s)$ for $s < 20$.

B. Statistical comparisons

A second question concerns the statistical testing of various hypotheses concerning the agreement or disagreement of our numerical estimates for $\bar{\rho}_D(s)$, for example, with either another set of such data or with a theoretical result. The difficulty with making such comparisons arises because of the serial correlation inherent in the MD method for computing time-correlation functions.

To make such a comparison in the presence of serial correlation, we compute the Hotelling T^2 statistic of multivariate statistical analysis.[32] Let the n by k matrix $\underline{Z}$, consisting of the n row vectors

$$\underline{z}_i = (z_{i1}, z_{i2}, \ldots, z_{ik}) \tag{5.1}$$

represent the observed velocity-autocorrelation function on trajectory i at times $t_1, t_2, \ldots, t_k$. Assuming the independence of the n vectors, we can test the hypothesis that the n observed $\underline{z}_i$ vectors, with mean and variance

$$\underline{y} = \frac{1}{n}\sum_{i=1}^{n} \underline{z}_i\ ,$$
$$\underline{S} = \frac{1}{n-1}\sum_{i=1} (\underline{z}_i - y)^{\dagger}(\underline{z}_i - y) \tag{5.2}$$

(where the dagger denotes the transpose) have been drawn from a normal population having mean $\underline{\xi}$ and unknown variance $\underline{\Sigma}$. For example, $\underline{\xi}$ might

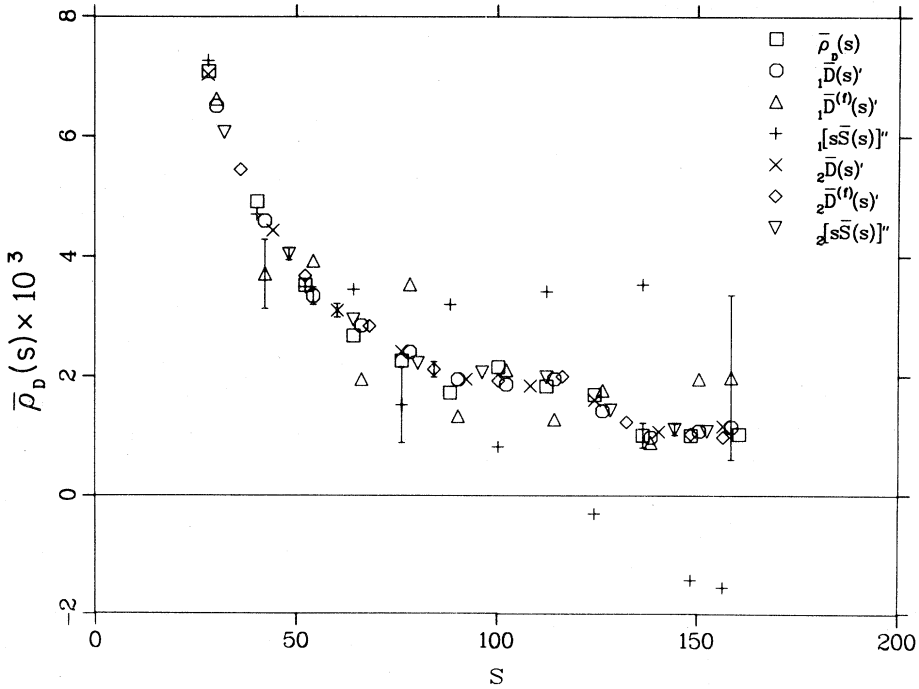

FIG. 1. Reduced VACF for a system of 5822 hard disks at a volume of $2V_0$ as a function of time s, in units of the mean-free time, computed: (1) directly (□); (2) from the time-dependent self-diffusion coefficients (○,△,×,◇), or (3) from the Einstein function (+,△). VACF's of types (2) and (3) are evaluated using central differences to approximate the derivatives, the leading subscript specifying the number of time-steps in the differencing interval.

consist of $\rho_D(t)$ at the k values of the time as given by the mode-coupling theory for finite N. Then T^2 is given by

$$T^2(n-1,k)=n(\underline{y}-\underline{\xi})\cdot\vec{\underline{S}}^{-1}\cdot(\underline{y}-\underline{\xi})^{\dagger} . \tag{5.3}$$

If the hypothesis is true, then

$$F=\frac{n-k}{k(n-1)}T^2(n-1,k) \tag{5.4}$$

has the so-called F distribution with k and $n-k$ degrees of freedom and we can evaluate the probability $P(T^2)$ that T^2 is no larger than the observed value. Values of $P(T^2)$ close to zero, say less than 0.05, indicate a better-than-expected agreement between $\underline{y}$ and $\underline{\xi}$. Values close to 1, say, less than 0.95, indicate a worse-than-expected agreement.

While $P(T^2)$ permits one to assess the probable validity of the theoretical $\underline{\xi}$, it does not bear on the ability of the test to reject the "null" hypothesis ($\underline{\xi}$) when the true mean is $\underline{\xi}'$. The latter depends on the power function[33]

$$P_\beta=1-\beta \tag{5.5}$$

in which

$$\begin{aligned}\beta&=P'_f(F',k,n-k,\varphi) ,\\ F'&=F(1-\alpha,k,n-k) ,\\ \varphi^2&=[n/(k+1)](\underline{\xi}'-\underline{\xi})\cdot\vec{\underline{\Sigma}}^{-1}\cdot(\underline{\xi}'-\underline{\xi})^{\dagger} ,\end{aligned} \tag{5.6}$$

where α is the level at which we agree to reject the null hypothesis that $\underline{\xi}$ is the true mean [i.e., we reject the hypothesis if $P(T^2)>1-\alpha$], $F(x,f_1,f_2)$ is the x fractile of the central F distribution for f_1 and f_2 degrees of freedom, and $P'_f(F',f_1,f_2,\varphi)$ is the cumulative distribution function for the noncentral F distribution with variate F', f_1, and f_2 degrees of freedom, and with noncentrality parameter φ. We note that the latter depends on the theoretical variance matrix $\underline{\Sigma}$. The quantity P_β, then, is the probability, given that $\underline{\xi}'$ is the true mean, that in testing the null hypothesis, we will in fact find T^2 such that $P(T^2)>1-\alpha$. Since we do not generally know the variance matrix $\underline{\Sigma}$, we cannot evaluate P_β exactly. For a given $\underline{\xi}'$ we can, however, obtain an approximate value by using the observed variance matrix $\underline{S}$ rather than $\underline{\Sigma}$. The power function depends, in addition, on the difference $\underline{\xi}-\underline{\xi}'$, as well as the level α, and the degrees of freedom k and $n-k$.

In applying the T^2 test and the power function, it is instructive to introduce an unknown "linear" parameter g, writing the theoretical mean

$$\underline{\xi}=g\underline{q} , \tag{5.7}$$

where, for the present comparison with the EHvL theory, $\underline{q}$ is the row vector formed by the k values of the theoretical $\rho_D(t)$ at times $t_1, t_2, \ldots, t_k$. In the case that one is comparing data with the limiting result, Eq. (1.1), the parameter g is a scale factor multiplying α_D, perhaps expected to arise from uncertainties with regard to which values to use for the transport coefficients. Under the null hypothesis, the parameter has a value $g_0=1$ for which we find

$$T^2=n(\underline{y}-g_0\underline{q})\cdot\vec{\underline{S}}^{-1}\cdot(\underline{y}-g_0\underline{q})^{\dagger} . \tag{5.8}$$

If we accept the $g=g_0$ hypothesis as true at the α level, then the power function against the alternative hypothesis $g=g_1$ is given by Eqs. (5.5) and (5.6), with noncentrality parameter

$$\varphi=|g_0-g_1|[n\underline{q}\cdot\vec{\underline{\Sigma}}^{-1}\cdot\underline{q}^{\dagger}/(k+1)]^{1/2} . \tag{5.9}$$

Again φ (and hence P_β) cannot be evaluated exactly, but if we replace $\underline{\Sigma}$ by $\underline{S}$ in Eq. (5.9), the resulting approximate values $\tilde{\varphi}$ and $\tilde{P}_\beta$ are expected to be useful. In particular, we can compute $\tilde{P}_\beta$ for a series of values of $\Delta g=|g_0-g_1|$ and denote that value of Δg for which $\tilde{P}_\beta$ is $1-\beta$ as $\Delta g_{1-\beta}$. In our applications of the test below, we report values of $\Delta g_{0.95}$, based on the rejection level $\alpha=0.05$. (The values of α and β, of course, need not have been chosen equal.) Thus if one rejects the EHvL theory as false when $P(T^2)>0.95$, and if the true mean value is $g_0\pm\Delta g_{0.95}$, then the probability of rejecting the theory is, very roughly, 0.95. We quote values of $\Delta g_{0.95}$ as a rough measure of the sensitivity of the "experimental" data to the variation of g.

Another statistical comparison which is frequently of value in treating MD data for time-correlation functions occurs when one has two distinct calculations having certain common parameters. An example might be the question of whether two realizations for the same density and system size using distinct calculational parameters (e.g., time-origin spacing) are in agreement. Thus, one might question whether two matrices of observations, say, the n_1 by k matrix $\underline{Z}^{(1)}$ and the n_2 by k matrix $\underline{Z}^{(2)}$, consisting of n_1 row vectors $\underline{z}_i^{(1)}$ and n_2 row vectors $\underline{z}_i^{(2)}$, respectively, representing the velocity-autocorrelation function at k values of the time with mean and variance $\underline{y}^{(j)}$ and $\underline{S}^{(j)}$ ($j=1,2$), have been drawn from normal populations having the same means $\underline{\xi}$ and unknown variances $\underline{\Sigma}^{(j)}$. For the case $\underline{\Sigma}^{(1)}=\underline{\Sigma}^{(2)}$, one computes[34]

$$T^2(n_1+n_2-2,k) = \frac{n_1 n_2}{n_1+n_2}(\underline{y}^{(1)}-\underline{y}^{(2)})\cdot\vec{\underline{S}}^{-1}\cdot(\underline{y}^{(1)}-\underline{y}^{(2)})^{\dagger},$$

$$\underline{S}=\frac{(n_1-1)\underline{S}^{(1)}+(n_2-1)\underline{S}^{(2)}}{n_1+n_2-2}, \tag{5.10}$$

while for the case $\underline{\Sigma}^{(1)}\neq\underline{\Sigma}^{(2)}$, taking $n_1\leq n_2$,[35]

$$T^2(n_1-k)=n_1(\underline{y}^{(1)}-\underline{y}^{(2)})\cdot\vec{\underline{S}}^{-1}\cdot(\underline{y}^{(1)}-\underline{y}^{(2)})^{\dagger},$$

$$\underline{S}=\frac{1}{n_1-1}\sum_{i=1}^{n_1}(\underline{w}_i-\underline{y})^{\dagger}(\underline{w}_i-\underline{y}), \tag{5.11}$$

where

$$\underline{w}_i=\underline{z}_i^{(1)}-\left[\frac{n_1}{n_2}\right]^{1/2}(\underline{z}_i^{(2)}-\underline{y}_1^{(2)})-\underline{y}^{(2)},$$

$$\underline{y}_1^{(2)}=\frac{1}{n_1}\sum_{i=1}^{n_1}\underline{z}_i^{(2)},$$

$$\underline{y}=\frac{1}{n_1}\sum_{i=1}^{n_1}\underline{w}_i=\underline{y}^{(1)}-\underline{y}^{(2)}.$$

Using Eq. (5.10) or (5.11) then, one can evaluate T^2 and compute $P(T^2)$ as above for the comparison with theory.

C. Trajectory precision

A third question of interest concerns the accuracy with which the trajectory is computed. It is well known[10] that a computer-generated trajectory will normally diverge from the true trajectory with increasing time. While it is possible to control the error by using multiple-precision arithmetic, it is common practice in MD to generate a very few (typically one) long trajectories, so that the computed trajectory bears little resemblance to the true trajectory except for a small portion near the initial time, the extent of which is determined by the calculational precision. It has been shown,[36] however, for so-called "Anosov" systems that there exists a true trajectory which in fact approximates the numerical trajectory, and that the numerical time average of a function of the phase approaches the time average on the neighboring trajectory, provided the trajectory is generated with sufficient accuracy. Subject to the validity of the quasiergodic hypothesis, the numerical time average approaches the ensemble average. While hard disks and spheres appear to belong to the Anosov class, the question remains as to what constitutes sufficient accuracy. In particular, one might well expect the trajectory calculation to require greater accuracy in order to estimate the VACF at long times than, say, to estimate the equation of state.

For hard-sphere and hard-disk systems, strong empirical evidence exists that the time average over a computer-generated trajectory approaches the true time average, inasmuch as there is agreement[10] between the numerical MD (Ref. 37) and MC (Ref. 38) equation-of-state results for hard spheres.[39] To study the question for the velocity-autocorrelation function empirically, we compare two calculations of the VACF, the first using double-precision arithmetic in the generation of the trajectory and the second using single-precision on the CDC-7600 computer which carries a 48-bit (about 14 digits) number in single precision. Both calculations are for a system of 5822 hard disks at a volume of $10V_0$. At this density, it is known[10] from a comparison of positions and velocities for such trajectories that the single-precision trajectory appears to have lost its accuracy completely after about ten mean-free times, i.e., the root-mean-square differences between the single-precision particle positions and velocities and the exact values appear to have reached their long-time limits. Nonetheless, the velocity-autocorrelation functions (computed from $_{\omega}[s\bar{S}(s)]''$), Fig. 2, remain in statistical agreement up to the $30t_0$ of the comparison. Using the T^2 test [Eq. (5.11)] to compare the two sets of data beyond

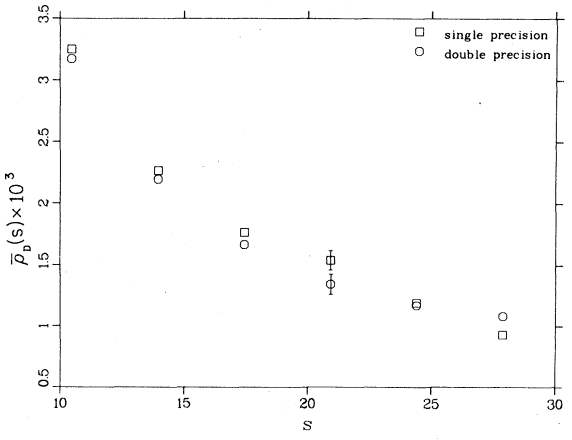

FIG. 2. Comparison of the reduced velocity-autocorrelation function for a system of 5822 hard disks at a volume of $10V_0$, computed both in double- (□) and single-precision (○) arithmetic, for values of the reduced time s greater than 10.

$10.5t_0$ yields $P(T^2)=0.55$. Thus, insofar as we can tell empirically, the loss of trajectory accuracy is not reflected in a loss of accuracy in the velocity-autocorrelation function.

VI. HARD DISKS: LONG-TIME BEHAVIOR

Table I lists the major parameters for the calculations of the velocity-autocorrelation function for

TABLE I. Parameters and mean-free time results for the Monte Carlo, molecular-dynamics calculations of the velocity-autocorrelation function of hard disks.[a]

V/V_0	N	P	$h/t_{00}^{(N)}$	ω	M	θ	N_c	t_0/t_{00}
30	1512	150	0.5	4	100	240	14	0.953 12±0.000 25
	1512	50	0.0953	20	40	3200	12	0.954 02±0.000 22[b]
20	1512	150	0.5	4	100	240	15	0.930 23±0.000 29
	1512	100	0.093	20	40	3200	24	0.930 15±0.000 17[b]
10	504	150	0.5	4	100	1000	22	0.862 33±0.000 20
	1512	150	0.5	4	100	240	16	0.861 23±0.000 21
	5822	118	0.5	6	102	240	48	0.860 91±0.000 12
	5822	119	0.5	3	51	300	60	0.860 91±0.000 11[c]
5	168	150	0.5	4	80	1440	12	0.727 18±0.000 24
	504	150	0.5	4	80	1440	37	0.728 61±0.000 13
	1512	150	0.2	5	150	600	19	0.728 29±0.000 15
	5822	50	0.2	10	150	600	24	0.727 93±0.000 13
3	168	400	0.2	10	150	1000	12	0.563 61±0.000 15
	168	384	0.2	10	150	1000	12	0.563 52±0.000 20
	504	190	0.2	10	150	600	10	0.561 94±0.000 15
	1512	160	0.2	5	150	600	26	0.561 57±0.000 11
	5822	50	1.5	1	40	100	39	0.561 45±0.000 09
	5822	50	0.2	10	150	600	31	0.561 45±0.000 09[b]
2	168	101	0.1	10	200	1000	2	0.373 77±0.000 21
	504	49	1.0	5	20	100	3	0.374 33±0.000 19
	1672	54	0.2	10	130	600	14	0.374 02±0.000 08
	4736	50	1.5	2	40	120	57	0.374 16±0.000 05
	5822	50	1.5	2	40	120	70	0.374 15±0.000 04
1.8	5822	66	1.5	2	40	120	109	0.317 77±0.000 03
1.6	5822	50	1.5	2	40	120	104	0.252 20±0.000 03
1.5	5822	50	1.5	2	40	120	122	0.215 66±0.000 02
	5822	50	0.1	4	80	400	27	0.215 76±0.000 04[b]
1.4	5822	50	1.5	2	40	120	148	0.177 36±0.000 02
	5822	50	0.1	4	80	400	33	0.177 35±0.000 05[d]
	5822	12	0.005	20	60	8000	8	c,d,b

[a]P is the number of trajectories, h is the time step, ω is the number of time steps per time origin, M is the number of time steps for the last value of VACF calculated, θ is the number of time steps per trajectory, N_c is the total number of collisions in millions, t_0 is the observed mean-free time, and $t_{00}^{(N)}$ and t_{00} are the low-density values for a finite system and an infinite system, respectively.

[b]Results for short times discussed in Sec. VII.

[c]Single-precision arithmetic for trajectory.

[d]Thermalization of 100 time steps used in initial phase generation.

hard disks, with reduced volumes ranging from $1.4V_0$ to $30V_0$. The observed mean-free time, with its associated standard deviation, is also given in the table. Except where indicated otherwise, all calculations are for the microcanonical ensemble, use double-precision (96 bits) arithmetic for the generation of the trajectory, and do not use initial thermalization. The VACF's obtained from these calculations[40] are reported in Figs. 3–9. In each figure, we plot the observed reduced velocity-autocorrelation function of the specified density for each system size N and at values of the time which are selected to permit much of the data to appear without overcrowding. The curves labeled EHvL are for the finite-N theory of Sec. III, using Enskog values for the transport coefficients and with the initial distribution-width parameter $\mu=0$. Also shown in many of these figures is the infinite system limit, labeled DC (for Dorfman and Cohen), Eq. (1.1), also based on the Enskog shear viscosity and self-diffusion coefficients. The arrows in the figures indicate the values of the acoustic-wave traversal time $t_a=L/c$ with the sound speed computed from the Padé (3×3) approximant, Eq. (4.13). For figures showing data for more than one system size, the smaller values of t_a refer to the smaller systems, although some values lie outside the displayed range of the time; such cases are discussed in the text. The dramatic effect of the finite-N theory in bringing the theory into approximate agreement with the data is evident. We note that for the most part the Alder-Wainwright[1] data were restricted to times smaller than those discussed here.

Table II shows the results of the T^2 comparison between the data and the modified EHvL theory. In making these comparisons, however, one expects the time interval (t_i,t_f) for which the comparison is made to be important. In particular, values of t_i which are too small would be expected to include in the interval times for which the mode-coupling theory is not valid. Indeed, one deficiency of the theory is the lack of an estimate of the time t_i at which it becomes valid. We are, therefore, in the position of having to estimate t_i from the results of our comparison. Thus, in Table II, these results are typically given for several different intervals (s_i,s_f) of the time (where $s=t/t_0$), with s_f the longest time for which data were calculated for the VACF. The smaller value (or values) of s_i usually is associated with a value of $P(T^2)$ near unity, indicating a probable disagreement between the theory and the data. That disagreement would, of course, be expected to worsen for even smaller values of s_i. The larger value of s_i typically has a value of $P(T^2)$ not

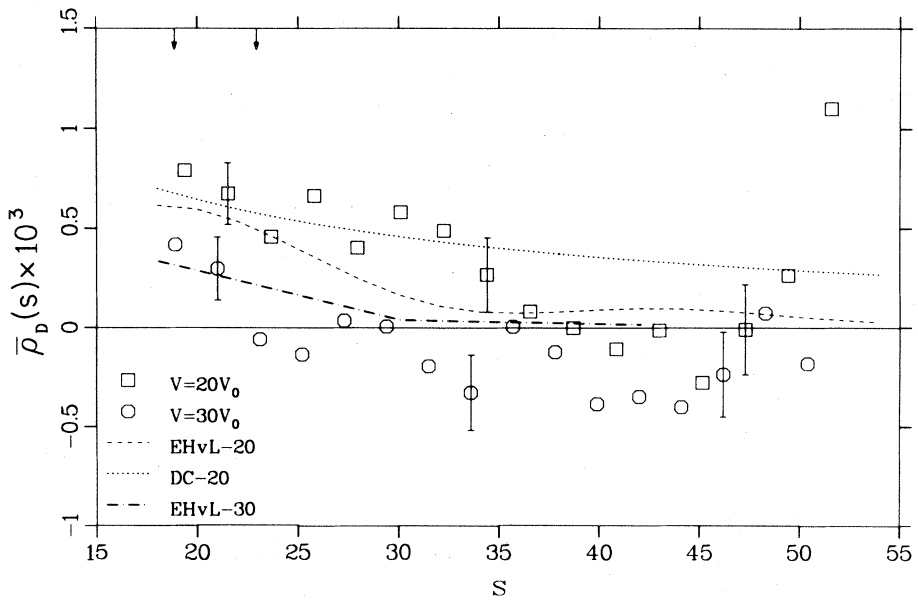

FIG. 3. Reduced velocity-autocorrelation function for 1512 hard disks at volumes of $20V_0$ (□) and $30V_0$ (○), as a function of the reduced time s. Curves show the theoretical results, with the asymptotic large-system result given by the dotted curve and the various dashed curves showing the finite-system mode-coupling theory. Arrows mark the values of the acoustic-wave traversal time.

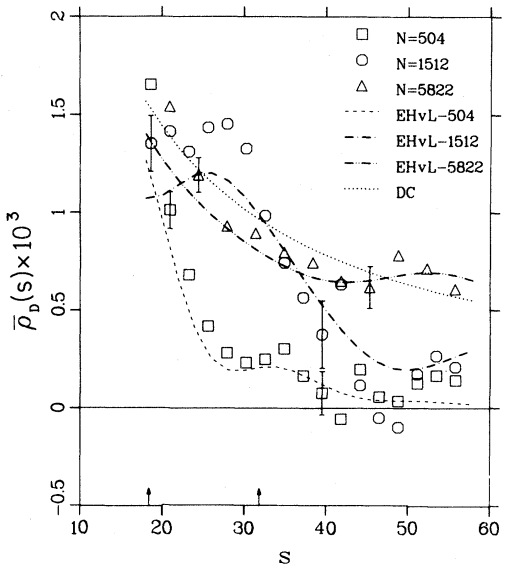

FIG. 4. Reduced velocity-autocorrelation function at a volume of $10V_0$, as a function of the reduced time s for systems of (□) 504, (○) 1512, and (△) 5822 hard disks. Curves are as in Fig. 3.

particularly near unity indicating probable agreement within the statistical uncertainty. These larger values of s_i in the table, then, are very crude estimates of the earliest times of agreement of our data with the theory. If our modification of the EHvL theory captures most of the finite-system effects at long times, then it would be expected that these values would be approximately independent of the system size and vary smoothly with the density. Finally the values of $\Delta g_{0.95}$ in the table indicate the sensitivity of the tests to the multiplicative factor g as discussed in Sec. V. We discuss each density separately, beginning with the lowest density.

The lowest-density results are shown in Fig. 3, for volumes of $30V_0$ and $20V_0$, both for 1512-particle systems; for each volume the data are those for the first realization listed in Table I. The value of t_a/t_0 (indicated by the arrows) for the $30V_0$ is smaller than for the higher-density system. Although a number of points lie more than a standard deviation from the EHvL curve, the T^2 test shows the difference to be unexceptional, as seen in Table II. Rather, the power of either set of data to distinguish among various theoretical curves is seen to be not very great, as evidenced by the very large values of $\Delta g_{0.95}$ in the table. The best that can be said in either case is that the data are consistent with the theory within, roughly, a multiplicative factor of 1 ± 2.6 for $30V_0$ and 1 ± 1.7 for $20V_0$.

For a volume of $10V_0$, the data are available for systems of 504, 1512, and 5822 particles. The data for all three systems are shown in Fig. 4. The acoustic-wave-traversal-time arrow for the 5822-particle system is well beyond the range of s in the figure. The 1512-particle data have large error bars and would not be expected to be as valuable in test-

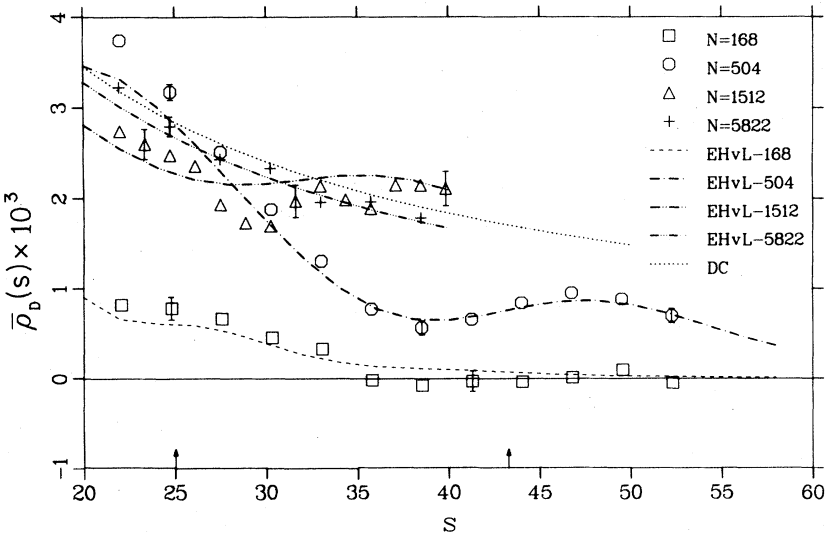

FIG. 5. Reduced velocity-autocorrelation function at a volume of $5V_0$, as a function of the reduced time s for systems of (□) 168, (○) 504, (△) 1512, and (+) 5822 hard disks. Curves are as in Fig. 3.

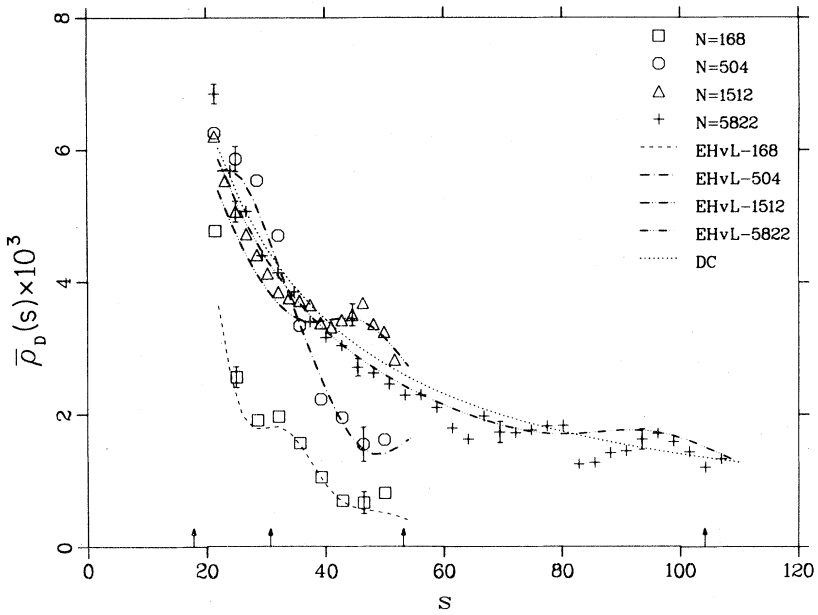

FIG. 6. Reduced velocity-autocorrelation function at a volume of $3V_0$, as a function of the reduced time s for systems of (□) 168, (○) 504, (△) 1512, and (+) 5822 hard disks. Curves are as in Fig. 3.

ing the theory as the other two systems. Nonetheless, the power of the T^2 test shown in Table II is not particularly different for that system. In any case, the differences between theory and the data are not significant provided we exclude the leftmost one or two of the plotted points from each comparison.

The VACF for four different sized systems are shown for a volume of $5V_0$ in Fig. 5. The values of t_a/t_0 for the 168- and 5822-particle systems are outside the range of s plotted. The T^2 comparisons in Table II show reasonable agreement for $N=168$ and 5822 for $t \geq 22t_0$. However, the more precise $N=504$ results appear to lie significantly above the theory unless $t \geq 27.5t_0$. The 1512-particle results are not as precise so that even though the data appear to have a deeper minimum near $30t_0$ than given by the theory, $P(T^2)$ is not especially large even for s_i as small as 19.2.

For the volume of $3V_0$, Fig. 6 shows results for the same four system sizes. In this case, however, for the 5822-particle system, the data extend to about $107t_0$ in the time, so that the time dependence of the theory is presumably better tested in this comparison. For 168 particles, the two realizations (see Table I) are combined in comparing with theory. It is seen from Table II that one must eliminate the first two plotted points from the T^2 comparison to obtain a reasonable value of $P(T^2)$. For $t_i \geq 28.5t_0$ the agreement is adequate. For $N=504$ the first four points lie more than a standard deviation above the theory. Not surprisingly, then, only for $t_i=35.6t_0$ do we observe reasonable values for $P(T^2)$. For the largest two systems, agreement is adequate for $t_i=24t_0$.

Consider next the volume $2V_0$, for which data for five system sizes are shown in Fig. 7. In Fig. 7(a) which gives results for the three smaller systems extending only to relatively short times, we note rather large discrepancies between the theory and the data. The 168- and 504-particle data consist of only a few points each because of the wide spacing of time origins in these calculations (see Table I). For the 168-particle system, only the point near $42t_0$ lies within one standard deviation of the theory, while neither of the two points for $N=504$ lie that close to the theoretical curve. For the 1672-particle system, the agreement with the theory seems somewhat questionable for the largest three values of the time. For this realization the T^2 test yields $P(T^2)=0.91$ for $t_i=37.4t_0$ and the value would not improve by restricting the comparison to even larger values of the time. We note that the 986-particle results of Alder and Wainwright[1] at times between $20t_0$ and $30t_0$ at this density appear to lie close to our 1672-particle results.

In Fig. 7(b), the results for the two largest systems, $N=4736$ and 5822, are displayed. We note

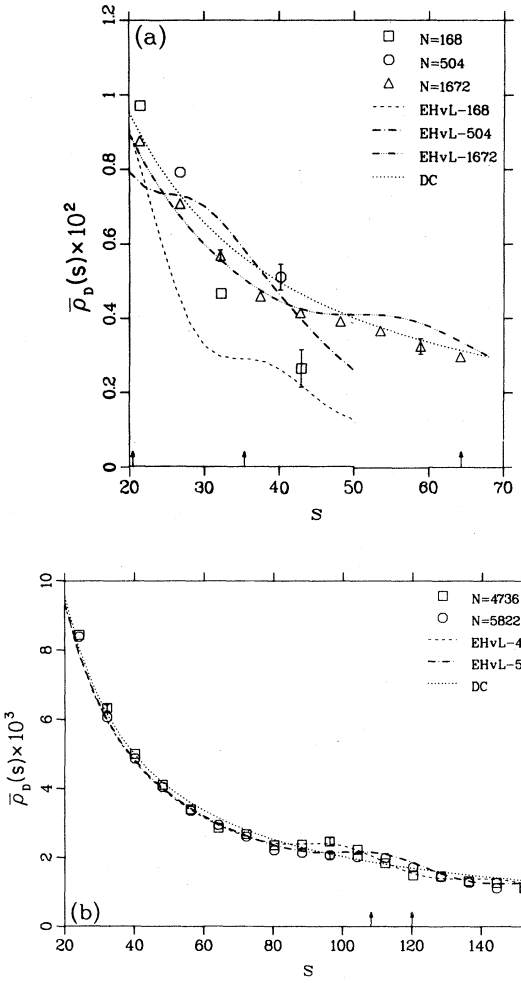

FIG. 7. Reduced velocity-autocorrelation function at a volume of $2V_0$, as a function of the reduced time s for systems of (a) (□) 168, (○) 504, (△) 1672, and (b) (□) 4736, (○) 5822 hard disks. Curves are as in Fig. 3.

that finite-system effects are small for these systems, as evidenced by the small difference between the DC curves and the finite-N curves. The results appear to agree well with either theory, except at the earliest times. Both sets of data yield reasonable values for T^2 for $t_i=40t_0$, although the 5822 results also agree at $t_i=32t_0$.

At the volume $V=2V_0$, then, except for the 1672-particle results, a consistent picture would result if we suppose that effects not of a hydrodynamic nature remain important up to about $40t_0$. Beyond that time, the mode-coupling theory and the data agree quite well. Moreover, the disagreement posed by the 1672-particle system is by no means serious in that for the time-interval (37.4,

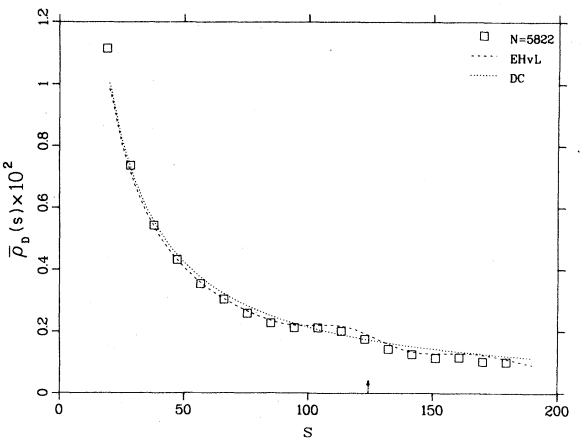

FIG. 8. Reduced velocity-autocorrelation function at a volume of $1.8V_0$, as a function of the reduced time s for a system of 5822 hard disks. Curves are as in Fig. 3.

65.1), $P(T^2)$ is 0.91, a value which is certainly not extraordinarily close to unity. Perhaps N-dependent terms not included in the theory become more important at this higher density, but the paucity of long-time data for the smaller systems [Fig. 7(a)] would make such a conclusion highly speculative.

For $V=1.8V_0$, the data in Fig. 8, which have rather small statistical uncertainties by virtue of the large number of collisions in the calculation, agree well with the theory for $t_i=37.8t_0$. From the T^2

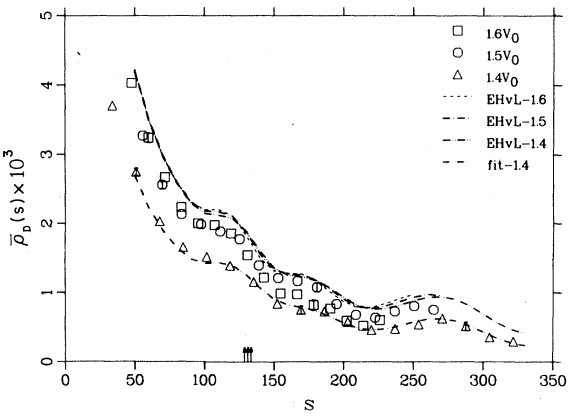

FIG. 9. Reduced velocity-autocorrelation function for systems of 5822 hard disks as a function of the reduced time s at volumes of (□) $1.6V_0$, (○) $1.5V_0$, and (△) $1.4V_0$. Curves are as in Fig. 3, except that the transport coefficients in the theoretical curve marked "fit" have been selected as in Eq. (6.1) in order to fit the $1.4V_0$ data.

TABLE II. Hotelling T^2 test results for hard disks, for comparison of MCMD results with the EHvL theory for finite N.

V/V_0	N	k	s_i	s_f	$P(T^2)$	$\Delta g_{0.95}$
30	1512	16	18.9	50.4	0.71	2.6
20	1512	16	19.4	51.6	0.72	1.0
		15	23.7	51.6	0.68	1.7
10	504	17	18.6	55.8	1.00	0.4
		16	20.9	55.8	0.54	0.6
10	1512	17	18.6	55.8	0.77	0.4
		16	20.9	55.8	0.69	0.5
10	5822	11	20.9	55.8	0.93	0.3
		10	24.4	55.8	0.26	0.3
5	168	13	19.2	52.2	0.99	0.6
		12	22.0	52.2	0.29	0.8
5	504	11	24.7	52.2	0.95	0.1
		10	27.5	52.2	0.85	0.2
5	1512	16	19.2	39.8	0.86	0.2
		14	22.0	39.8	0.89	0.2
		12	24.7	39.8	0.91	0.2
5	5822	8	19.2	38.5	0.94	0.2
		7	22.0	38.5	0.46	0.2
3	168	8	24.9	49.9	0.98	0.2
		7	28.5	49.9	0.71	0.2
3	504	6	32.1	51.7	0.98	0.2
		5	35.6	51.7	0.64	0.3
3	1512	18	21.4	51.7	0.92	0.1
		16	24.9	51.7	0.57	0.1
3	5822	32	24.0	106.9	0.90	0.1
		31	26.7	106.9	0.87	0.1
2	168	3	21.4	42.8	0.99	0.3
		2	32.1	42.8	0.99	0.7
2	504	2	31.5	47.2	0.81	0.2
2	1672	7	32.1	64.1	0.96	0.1
		6	37.4	64.1	0.91	0.1
2	4736	16	32.1	152.4	0.97	0.1
		15	40.1	152.4	0.82	0.1
2	5822	17	28.3	152.4	1.00	0.1
		16	32.1	152.4	0.50	0.1
		12	75.5	152.4	0.58	0.1

TABLE II. *(Continued.)*

V/V_0	N	k	s_i	s_f	$P(T^2)$	$\Delta g_{0.95}$
1.8	5822	17	28.3	179.4	1.00	0.05
		16	37.8	179.4	0.41	0.08
		12	75.5	179.4	0.58	0.1
1.6	5822	17	35.7	225.8	1.00	0.08
		14	71.3	225.8	0.96	0.1
1.5	5822	14	83.3	263.9	1.00	0.1
1.4	5822	14	101.6	321.7	1.00	0.1
		17	50.8	321.7	0.81	0.1[a]

[a]EHvL based on transport coefficients $D=1.6D_E$, $\eta=1.5\eta_E$, $\lambda=1.2\lambda_E$, and $\zeta=1.2\zeta_E$.

comparisons in Table II, we see that the fact that each data point lies below the theoretical curve for $t>75t_0$ is not significant in light of the serial correlation in the data, even when the comparison is limited to that interval.

For the three highest densities studied, viz., $V=1.6, 1.5$, and $1.4V_0$, the VACF for 5822 particles are shown in Fig. 9. We see that the data lie below the finite-N mode-coupling result and that the difference increases with increasing density. In each case, the difference is statistically significant and extends to such long times that it would not appear to arise from a slowly decaying transient. One can attempt to bring the mode-coupling theory into agreement by using values of the transport coefficients other than the Enskog values. Indeed, there is no fundamental reason to use the Enskog values and an approach in which values given by the time integral of the appropriate time-correlation function [for example, the $t\to\infty$ of Eq. (2.3b), provided the limit exists, as suggested by both the MD results and the theory of Sec. III] for the finite system might seem appropriate. However, for these high densities, the time-dependent transport coefficients have not reached a limiting value even at $250t_0$ for $V=1.4V_0$. One can, however, empirically find values which bring the theory into agreement with the data, as shown by the curve labeled "fit" in Fig. 9, for which we used

$$D=1.6D_E,\quad \eta=1.5\eta_E\ ,\qquad \lambda=1.2\lambda_E,\quad \zeta=1.2\zeta_E\ . \tag{6.1}$$

These values are similar to our unpublished molecular-dynamics values for this same system, except that η is about 10% lower than given in Eq. (6.1). The fit is not sensitive to the value of D at this density. In any case, the use of transport coefficients larger than the Enskog values does seem to move the mode-coupling results in the right direction. If finite-system values were known for these coefficients over the entire fluid range, it would be of interest to repeat the present comparison using these values.

VII. HARD DISKS: SHORT AND INTERMEDIATE TIMES

At values of the time earlier than those discussed in Sec. VI, we present our results relative to the Lorentz-Boltzmann-Enskog theory which is to first order in the Sonine polynomial expansion[41]

$$[\rho_D(t)]_1=(\beta m)^{-1}\exp(-2s/d) \tag{7.1}$$

and which is to fifth order given by[42]

$$[\rho_D(t)]_5=(\beta m)^{-1}\times\sum_{l=0}^{4}B_l\lambda_l\exp(-\lambda_l s)\ . \tag{7.2}$$

The B_l and λ_l are given in Table III for hard spheres and disks. Because the relations

$$\sum_{l=0}^{4}B_l\lambda_l=1\ ,\qquad \sum_{l=0}^{4}B_l\lambda_l^2=2/d\ , \tag{7.3}$$

hold,[42] it follows that Eqs. (7.1) and (7.2) are equal and have equal first derivatives at $t=0$. The second derivative of Eq. (7.2) yields values in agree-

TABLE III. Coefficients for the Lorentz-Boltzmann-Enskog theory for the velocity-autocorrelation function of hard spheres and disks, in the fifth Enskog approximation.

d	l	B_l	λ_l
2	0	$4.401\,418\,682\times10^{-1}$	1.076 378 065
	1	$5.413\,144\,648\times10^{-1}$	0.846 022 9532
	2	$4.440\,122\,403\times10^{-2}$	1.483 431 123
	3	$1.181\,558\,688\times10^{-3}$	2.029 232 317
	4	$4.669\,244\,312\times10^{-6}$	2.713 877 712
3	0	$2.299\,809\,059\times10^{-1}$	0.809 617 833
	1	$5.754\,347\,358\times10^{-4}$	1.499 170 956
	2	1.274 318 433	0.617 599 688
	3	$2.353\,397\,056\times10^{-2}$	1.101 796 540
	4	$1.907\,528\,804\times10^{-6}$	2.014 824 180

ment with the exact Enskog values of de Schepper, Ernst, and Cohen[17] to seven significant figures.

In presenting data in the early-to-intermediate time regime, we take advantage of the empirical observation that the $c_D(t)$ correlation function is largely independent of system size at early times. This can be seen in Fig. 10 which shows the functions

$$\begin{aligned}\Delta\bar{\rho}_D(s)&=\bar{\rho}_D(s)-[\bar{\rho}_{DE}(s)]_5\,,\\ \Delta\bar{c}_D(s)&=\bar{c}_D(s)-[\bar{\rho}_{DE}(s)]_5\,,\\ [\bar{\rho}_{DE}(s)]_5&=(t_0/D_E)[\rho_{DE}(st_0)]_5\,,\end{aligned}\tag{7.4}$$

for a volume of $10V_0$ for systems of 504, 1512, and 5822 particles. The second function appears to be much less dependent on N for small values of s. [A similar $O(1/N)$ "correction" was applied by Alder and Wainwright.[1]] The same appears true at $V=5V_0$, $3V_0$, and $2V_0$. Therefore, we present results for $\Delta\bar{c}_D(s)$ only for the largest systems for which we have made calculations, in the belief that for these times these represent results near the infinite-system limit. [The calculation of $\Delta\bar{c}_D(s)$ for these and subsequent results is based on Eq. (2.5), using the observed estimates for $\langle P^2\rangle$ rather than the exact value. This procedure appears to minimize the fluctuations in this quantity.]

The short-time behavior of the VACF has been considered theoretically by de Schepper and Cohen[43] and de Schepper, Ernst, and Cohen[17] who have computed the leading (linear) term in the time and obtained the quadratic term in terms of the equilibrium three-particle correlation function at contact. The t^2 term then has been evaluated exactly in the low-density limit and approximately at all densities for hard spheres by de Schepper, Ernst, and Cohen.[17] The linear term involves the dynamics of a single collision and can be evaluated exactly for the NVE ensemble (for a finite periodic system), yielding

$$c_D(0)'=-\frac{2}{d\beta mt_0}\frac{Nd}{Nd+1}\,,\tag{7.5}$$

where t_0 is the NVE-ensemble collision rate

$$\begin{aligned}t_0&=\frac{\pi^{1/2}G(Nd/2,\frac{1}{2})(\beta m)^{1/2}}{n\sigma^{d-1}\omega_d\bar{g}_{NV}(\sigma)}\,,\\ \omega_d&=2\pi^{d/2}/\Gamma(d/2)\,,\\ G(M,m)&=\Gamma(M+m)/M^m\Gamma(M)\,,\end{aligned}\tag{7.6}$$

where $\bar{g}_{NV}(r)$ is the angle-averaged pair-correlation function. For early times, then, we find

$$\Delta\bar{c}(s)=\frac{2t_0}{d\beta mD_E}\frac{1}{Nd+1}s+F_ds^2+O(s^3)\tag{7.7}$$

with F_d given by de Schepper and Cohen in the thermodynamic limit as an integral involving the triplet correlation function at contact, given explicitly in the low-density limit,[17] viz.,

$$\begin{aligned}F_2&=[t_0/(\beta mD_E)][0.003\,517-0.005\,858(V_0/V)+\cdots]\,,\\ F_3&=[t_0/(\beta mD_E)][0.108\,928-0.010\,60(V_0/V)+\cdots]\,.\end{aligned}\tag{7.8}$$

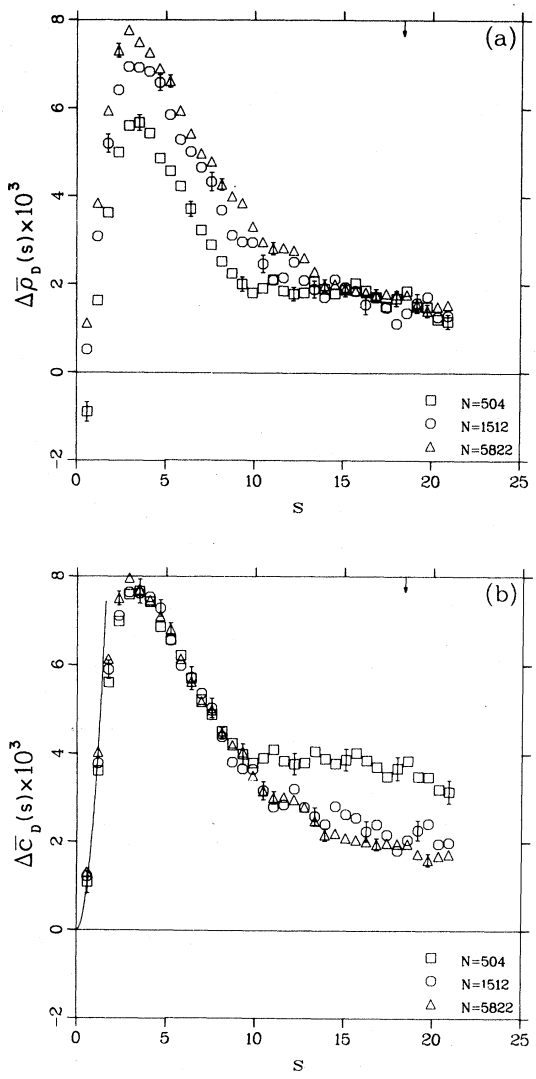

FIG. 10. Difference between the reduced velocity-autocorrelation function and the Lorentz-Boltzmann-Enskog theory as a function of the reduced time s at a volume of $10V_0$ for systems of (□) 504, (○) 1512, and (△) 5822 hard disks. (a) Shows the VACF in the center-of-mass frame of reference while (b) shows the VACF in the laboratory frame of reference. Solid curve in the latter is the theoretical early time behavior, Eq. (7.7), for $N=5822$.

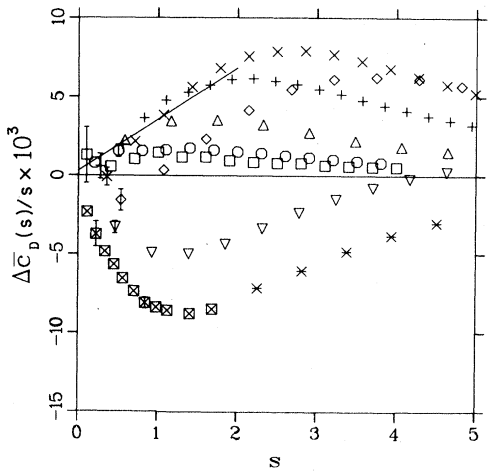

FIG. 11. Plot of the difference between the reduced velocity-autocorrelation function and the Lorentz-Boltzmann-Enskog theory, divided by the reduced time s for hard disks at volumes of (□) 30, (○) 20, (△) 10, (+) 5, (×) 3, (◇) 2, (△) 1.5, and (⊠), (✳) 1.4 times the close-packed volume V_0.

This theoretical curve (using $N=5822$) is shown in Fig. 10(b) for $V=10V_0$, but the curve is very steep at the early times at which there is at least qualitative agreement.

In Fig. 11 we plot $\Delta\bar{c}(s)/s$ as a function of s for eight different densities up to a time $s\approx5$. For volumes of 30, 20, 3, 1.5, and $1.4V_0$, the data are from the second (or second and third for 1.4) realization given in Table I for that volume and for the largest value of N. Also shown is the theoretical zero-density line, Eqs. (7.7) and (7.8), using $N=1512$ to evaluate the $s=0$ intercept, corresponding to the system size for the lowest two densities in the figure. Evidently the data are consistent with the exact [except for $O(1/N)$ corrections] low-density slope, but the large error bars for small s do not warrant a quantitative comparison. A more extensive low-density calculation taking data at smaller increments in s would appear to be needed in order to verify agreement with the de Schepper-Cohen result.

A calculation in which results were obtained at small values of the time has been made at the highest density, viz., $V=1.4V_0$, with only every fourth point shown in Fig. 11, but with every point shown in Fig. 12 up to $s\approx\frac{1}{2}$. The calculational parameters for this system are given in Table I, but variable spacing of observation times was employed, viz., $\{n\}=\{20,4,2\}$ and $\{k\}=\{1,5,10\}$. While ordinary least squares is not appropriate for the determination of the initial slope, correlated least squares can be applied, provided the covariance matrix for the observations is known.[44] Although the latter is not known, a rough estimate for it can be obtained from the observed covariance matrix for the 12 trajectories generated for this realization. Using the latter and fitting the ten data points $s=0.0563, 0.1126, \ldots, 0.5634$ (alternate points in

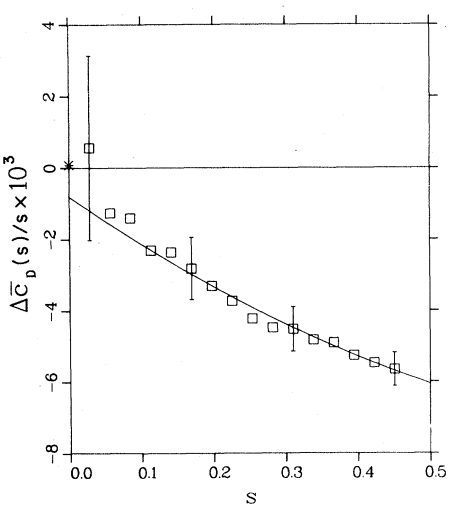

FIG. 12. Plot of the difference between the reduced velocity-autocorrelation function and the Lorentz-Boltzmann-Enskog theory, divided by the reduced time s for 5822 hard disks at a volume of $1.4V_0$ at small values of the reduced time s. Solid curve is a correlated-least-squares quadratic fit, given by Eqs. (7.9) and (7.10). ($\times$) marks the exact theoretical intercept, given in Eq. (7.7).

the figure) to a quadratic in s,

$$\Delta\bar{c}(s)/s = a + bs + cs^2 \tag{7.9}$$

one obtains

$$\begin{aligned} a &= -0.000\,81 \pm 0.000\,85\ , \\ b &= -0.014\,00 \pm 0.002\,06\ , \\ c &= 0.007\,03 \pm 0.001\,40\ , \end{aligned} \tag{7.10}$$

where the uncertainties are one standard deviation. We note, however, because these standard deviations have only two degrees of freedom they have little precision. This curve is also plotted in Fig. 12. A calculation using neighboring values of the time, viz., $s = 0.0282, 0.0845, \ldots, 0.5352$, yields values for the coefficients consistent with these. We note that the value of the intercept a is marginally consistent with the exact value of 0.000 08 given by Eq. (7.7), which is also plotted in the figure. Unfortunately no value for the de Schepper-Cohen coefficient is available at this density with which to compare the value of b.

In the intermediate time regime, say from 5 to 20 mean-free times, we present results for $\Delta\bar{c}_D(s)$ only for the largest systems available. In Fig. 13(a) we plot the results for the five lowest densities from $V = 30V_0$ to $V = 3V_0$, showing the increasingly large deviations from the Enskog theory, independent of the divergence arising from the long-time tail. In Fig. 13(b) the five highest densities ($V = 2V_0$ to $V = 1.4V_0$) show the reverse trend, with negative deviations near five mean-free times.

VIII. DISCUSSION

The calculation of the velocity-autocorrelation function for hard spheres and disks serves in many ways as a prototype for calculations of other time-correlation functions and for more complicated interaction potentials. One expects to be able to obtain greater precision for hard-core systems and be able, therefore, to obtain more definitive results both with respect to questions of methodology as well as questions of physics.

We have, therefore, addressed two types of questions in this paper. First, we have considered a number of methodological questions, which would appear to have general applicability in the calculation of time-correlation functions. While the discussion and results in Sec. V are not necessarily definitive, they should prove valuable in the context of most such calculations.

Second, we have presented VACF results for many densities and system sizes, particularly with a view toward testing the validity of the mode-coupling theory, although results are presented at short times as well. The current test of the mode-coupling theory is extensive, particularly in that we are able to extend the comparison to times beyond the acoustic-wave traversal time, which signals the beginning of strong system-size effects. While the support for the theory is not very strong in the low-density regime, the comparisons reported in Table II and in Figs. 4–8 provide strong support for the validity of the mode-coupling theory. The high-density comparison (Fig. 9) signals an important weakness of the theory by not providing an unequivocal prescription for the "bare" transport coefficients. This, together with the lack of some estimate of what values of the time the theory should become valid, seem to be problems which should be addressed by the theory.

The short-time results seem particularly interesting in the form of the correction to the Lorentz-Boltzmann-Enskog theory. The lack of results at very short time and low densities has prevented us from making contact with the exact theoretical results of de Schepper and Cohen.[43] The structure, particularly the maximum, seen in Fig. 11 would appear to be especially interesting theoretically.

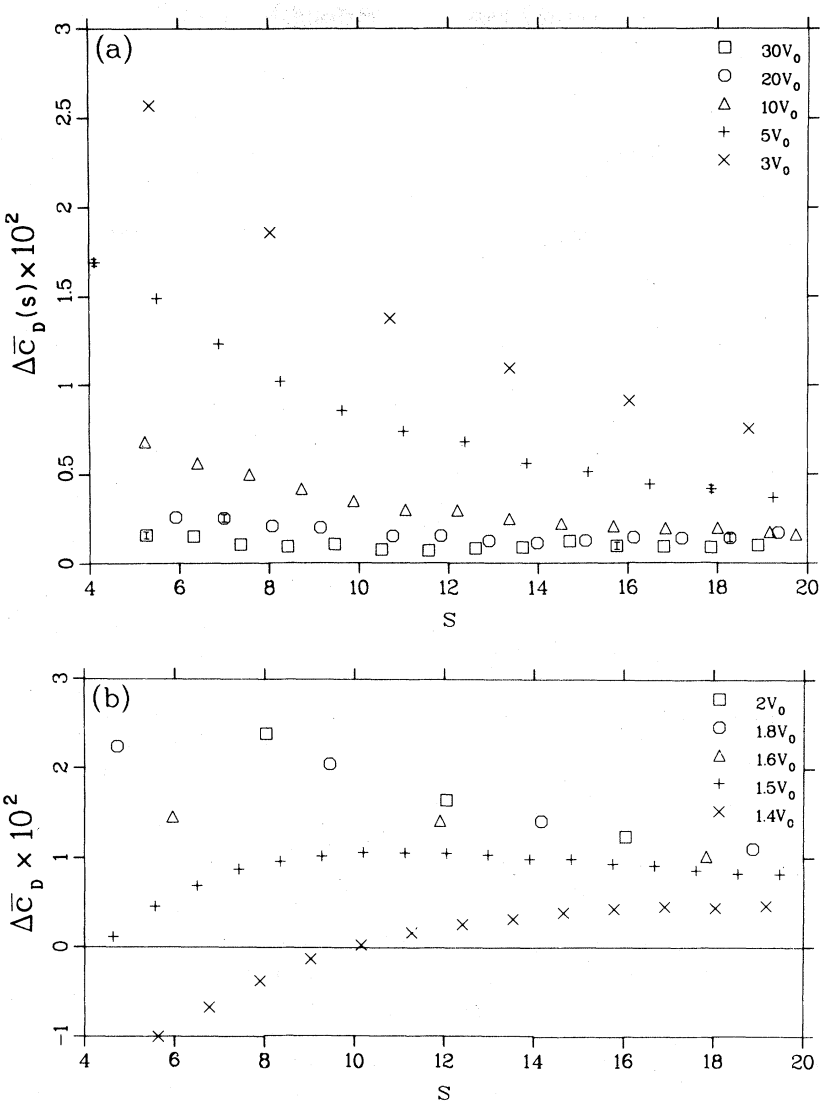

FIG. 13. Difference between the reduced velocity-autocorrelation function and the Lorentz-Boltzmann-Enskog theory as a function of the reduced time s for intermediate values of the time for volumes of (a) (□) 30, (○) 20, (△) 10, (+) 5, (×) 3, and (b) (□) 2, (○) 1.8, (△) 1.6, (+) 1.5, (×) 1.4 times the close-packed volume V_0.

ACKNOWLEDGMENTS

The authors wish to acknowledge several useful discussions over the several years which span the duration of this work. Contributors include E. G. D. Cohen, J. R. Dorfman, I. M. de Schepper, M. H. Ernst, J. D. Johnson, B. L. Holian, B. J. Alder, T. E. Wainwright, and J. L. Lebowitz. We are most appreciative of their help. This work was performed under contract with the U. S. Department of Energy.

APPENDIX

For the sake of completeness, we list here the coefficient matrix $\underline{\tilde{M}}_k$ which appears in the linearized hydrodynamic equations in $\vec{k}$ space.

$$\underline{\tilde{M}}_k = \begin{bmatrix} 0 & -in\vec{\kappa} & 0 \\ -\frac{ic^2}{\gamma n}\vec{\kappa} & -\nu\kappa^2\underline{I}_d - (D_l - \nu)\vec{\kappa}\vec{\kappa} & -\frac{ic^2\alpha}{\gamma}\vec{\kappa} \\ 0 & -\frac{i(\gamma-1)}{\alpha}\vec{\kappa} & -\gamma D_T\kappa^2 \end{bmatrix}, \tag{A1}$$

where $\underline{I}_d$ is the d-dimensional unit matrix. Simplification of the equations by the elimination of the $\vec{u}^{\parallel}$ equation yields Eq. (3.24) in which

$$\underline{Q}_k = \begin{bmatrix} 0 & -in & 0 \\ -\frac{ic^2}{\gamma n} & -D_l\kappa & -\frac{ic^2\alpha}{\gamma} \\ 0 & -\frac{i(\gamma-1)}{\alpha} & -\gamma D_T\kappa \end{bmatrix}. \tag{A2}$$

---

*Present address: Carroll College, Helena, Montana 59601.

[1]B. J. Alder and T. E. Wainwright, Phys. Rev. Lett. 18, 988 (1967); Phys. Rev. A 1, 18 (1970).

[2]J. R. Dorfman and E. G. D. Cohen, Phys. Rev. Lett. 25, 1257 (1970); Phys. Rev. A 6, 776 (1972); 12, 292 (1975).

[3]M. H. Ernst, E. H. Hauge, and J. M. J. van Leeuwen, Phys. Rev. Lett. 25, 1254 (1970); Phys. Rev. A 4, 2055 (1971).

[4]M. H. Ernst, E. H. Hauge, and J. M. J. van Leeuwen, J. Stat. Phys. 15, 7 (1976); 15, 23 (1976).

[5]K. Kawasaki, Prog. Theor. Phys. Jpn. 45, 1691 (1971); 46, 1299 (1971).

[6]Y. Pomeau, Phys. Rev. A 5, 2569 (1972); 7, 1134 (1973); Phys. Lett. 38A, 245 (1972).

[7]Y. Pomeau and P. Resibois, Phys. Rep. 19, 63 (1975).

[8]W. W. Wood, Acta Phys. Austriaca Suppl. X, 451 (1973).

[9]W. W. Wood, in *Fundamental Problems in Statistical Mechanics III,* edited by E. G. D. Cohen (North-Holland, Amsterdam, 1975), pp. 331–388.

[10]J. J. Erpenbeck and W. W. Wood, in *Modern Theoretical Chemistry, Vol. 6, Statistical Mechanics, Part B, Time-Dependent Processes,* edited by B. J. Berne (Plenum, New York, 1977).

[11]J. J. Erpenbeck and W. W. Wood, J. Stat. Phys. 24, 455 (1981).

[12]D. Lieberworth and E. G. D. Cohen, Phys. Lett. 58A, 209 (1976).

[13]I. M. de Schepper and E. G. D. Cohen, Phys. Lett. 68A, 308 (1978).

[14]J. V. Sengers, D. T. Gillespie, and J. J. Perez-Esandi, Physica (Utrecht) 90A, 365 (1978).

[15]I. M. de Schepper and M. H. Ernst, Physica (Utrecht) 93A, 611 (1978).

[16]E. G. D. Cohen and I. M. de Schepper, in *Fundamental Problems in Statistical Mechanics IV,* edited by E. G. D. Cohen and W. Fiszdon (Zaklad Narodowy im. Ossolinskich, Wroczlaw, Poland, 1978), pp. 101–160.

[17]I. M. de Schepper, M. H. Ernst, and E. G. D. Cohen, J. Stat. Phys. 25, 321 (1981).

[18]M. H. Ernst and H. van Beijeren, J. Stat. Phys. 26, 1 (1981).

[19]B. Kamgar-Parsi and J. V. Sengers, Proceedings of the Eighth Symposium on Thermophysical Properties (American Society of Mechanical Engineers, New York, in press).

[20]T. Keyes and B. Ladanyi, J. Chem. Phys. 62, 4787 (1975).

[21]In actual fact, the hard-sphere systems for which we have results are all cubic, while the hard-disk systems are rectangular. Because the differences in edge lengths for the hard-disk systems are never greater than 1.0%, this simplification to a d-dimensional cube has only a trivial effect on the reported predictions of the theory for the systems of interest.

[22]N. G. De Bruijn, *Asymptotic Methods in Analysis* (North-Holland, Amsterdam, 1958), p. 52.

[23]I. S. Gradshteyn and I. M. Ryzhik, *Table of Integrals, Series and Products* (Academic, New York, 1965), p. 495.

[24]W. W. Wood and J. J. Erpenbeck, J. Stat. Phys. 27, 37 (1982).

[25]W. W. Wood, in *Physics of Simple Liquids,* edited by H. N. V. Temperley, J. S. Rowlinson, and G. S. Rushbrooke (North-Holland, Amsterdam, 1968), pp. 116–230.

[26]B. Jansson, *Random Number Generators* (Pettersons, Stockholm, 1966).

[27]C. L. Pekeris, Proc. Natl. Acad. Sci. 41, 661 (1955).

[28]S. Chapman and T. G. Cowling, *The Mathematical*

Theory of Non-uniform Gases, 3rd ed. (Cambridge University Press, London, 1970).

[29]F. H. Ree and W. G. Hoover, J. Chem. Phys. 40, 939 (1964).

[30]D. M. Gass, J. Chem. Phys. 54, 1898 (1971).

[31]This behavior has its origin in the appearance of $u_{1x}(t)$ in Eq. (4.5) whereby the serial correlation between $\bar{D}^{(f)}(s)$ and $\bar{D}^{(f)}(s+h)$ is strongly affected by whether or not s is a time origin. For an example of a time-correlation function behaving similiarly, but with the effect magnified, see Ref. 10.

[32]T. W. Anderson, *An Introduction to Multivariate Statistical Analysis* (Wiley, New York, 1958), pp. 101–112.

[33]T. W. Anderson, Ref. 32, pp. 112–115.

[34]T. W. Anderson, Ref. 32, pp. 108–109.

[35]T. W. Anderson, Ref. 32, pp. 118–120.

[36]G. Benettin, M. Casartelli, L. Galgani, A. Giorgilli, and J. M. Strelcyn, Nuovo Cimento 44, 183 (1978); 50, 211 (1979).

[37]W. G. Hoover and B. J. Alder, J. Chem. Phys. 46, 686 (1967).

[38]W. W. Wood, Los Alamos Scientific Laboratory Report No. LA-2827, 1963 (unpublished).

[39]This is not to ignore the problem of the precision of the MC calculation, analogous to the MD problem. Rather, we suppose that the effects of precision should not affect the MC and MD results for the equation of state in the same way, so that the apparent agreement of the results of the two methods supports the hypothesis that the effects of precision on the equation of state is inconsequential at the level of statistical uncertainty achieved in these calculations.

[40]See AIP document No. PAPS PLRAA-26-1648-26 for 26 pages of tabular results for the velocity autocorrelation obtained in these calculations. Order by PAPS number and journal reference from American Institute of Physics, Physics Auxiliary Publication Service, 335 East 45th Street, New York, N. Y. 10017. The price is $1.50 for a microfiche, or $5.00 for a photocopy. Airmail additional. Make checks payable to the American Institute of Physics.

[41]B. J. Alder, D. M. Gass, and T. E. Wainwright, J. Chem. Phys. 53, 3813 (1970).

[42]W. W. Wood and J. J. Erpenbeck (unpublished).

[43]I. M. de Schepper and E. G. D. Cohen, Phys. Lett. 55A, 385 (1976); 56A, 499 (1976).

[44]T. W. Anderson, *The Statistical Analysis of Time Series* (Wiley, New York, 1971), pp. 18–20.